**Daining Fang**
Department of Engineering Mechanics,
Tsinghua University,
Beijing 100084, P.R.C.
e-mail: fangdn@mail.tsinghua.edu.cn

**Yongping Wan**
School of Aerospace Engineering
and Applied Mechanics,
Tongji University,
Shanghai 200092, P.R.C.;
Department of Engineering Mechanics,
Tsinghua University,
Beijing 100084, P.R.C.

**Xue Feng**
Department of Engineering Mechanics,
Tsinghua University,
Beijing 100084, P.R.C.

**Ai Kah Soh**
Department of Mechanical Engineering,
University of Hong Kong,
Hong Kong, P.R.C.

# Deformation and Fracture of Functional Ferromagnetics

*This article presents an overview of recent progress on magnetomechanical deformation and fracture of functional ferromagnetic materials. Following a brief introduction of the classical magnetoelasticity and the magnetomechanical behavior of traditional ferromagnetics, recent development on the deformation and fracture of soft ferromagnetic materials and the mechanics of ferromagnetic composites is critically reviewed. Also included are the authors' own works both on experimental testing and theoretical modeling of soft ferromagnetics, ferromagnetic composites, and shape memory ferromagnetic alloys. This review article cited 162 references.* [DOI: 10.1115/1.2888519]

*Keywords: magnetomechanics, deformation, fracture, composites, magnetoelastic experiment*

## 1 Introduction

Due to the widespread use of ferromagnetic materials in practical engineering, it has become increasingly important to explore their mechanical behavior under external magnetic field [1]. Ferromagnetic steel, for example, is a typical soft ferromagnetic widely used in nuclear reactors, and the analysis of its magnetoelastic performance has always been an important aspect of the structural analysis in the design of a nuclear reactor [2–8]. With scientific and technological advances in the past few decades, many new types of functional ferromagnetic material emerge, such as the giant magnetostrictive alloy of rare earth (RE) elements and iron [9,10], magnetostrictive composites [11–13], and ferromagnetic shape memory alloys [14–18]. Due to their superior properties, the new ferromagnetics have been employed to make sensors, actuators, and transducers. Correspondingly, the field of magnetomechanics has substantially grown.

Many researchers have contributed to the understanding of the classical mechanics of ferromagnetic structures. One of the main research subjects of traditional ferromagnetoelasticity has been the magnetoelastic buckling of ferromagnetic plates. Representative works on this subject are reviewed below.

Panovko and Gubanova [19] initiated the study on the stability of a ferromagnetic beam subjected to a static external magnetic field. Moon et al. [20–23] systematically studied the mechanical behavior of ferromagnetic plates and inductance winding structures. Their experiments revealed, for the first time, the magnetoelastic buckling of a ferromagnetic plate under a transverse magnetic field. Supposing that the magnetic field distributes homogeneously in the plate, they also developed a theoretical model, which gives an approximate result agreeing with experiment data when the ratio of plate length to thickness is relatively large. By means of the perturbation method, Pao and co-workers [24,25] established a linearized magnetoelastic theory on the basis of general nonlinear theory for multidomain soft ferromagnetic continuum subjected to a quasistatic magnetic field [2]. This linearized magnetoelastic theory was obtained from the general coupled field equations, boundary conditions, and nonlinear constitutive equations. Eringen [6,26] and Maugin [5] combined electroelasticity with magnetoelasticity to establish a general theory of magnetoelectroelastic continuum. Miya et al. [27,28] calculated the distribution of magnetic field in magnetic materials by means of the finite element method. They also conducted experiments to study buckling of ferromagnetic plates with different length to thickness ratios. By using a variational formulation, Van de Ven [29,30] and Lieshout et al. [31] derived the same theoretical result as that of Pao and Yeh [24]. For the ferromagnetics with low susceptibility and high thermal conductivity, Takagi and Tani [32] applied the modal magnetic damping method in the magnetomechanical analysis of a vibrating thin plate in a magnetic field, and found that this method gives a conservative evaluation in structural design in a strong magnetic field. Xie et al. [33] studied the size effect on the magnetoelastic buckling of a ferromagnetic plate under an external magnetic field. Zhou, Zheng, and co-workers [34–40], and Zhou and Miya [41] systematically investigated the buckling of a soft ferromagnetic plate under a magnetic field. They developed a new model of magnetic forces to interpret the experimentally observed increase of natural frequencies under a longitudinal magnetic field. Yang et al. [42,43] proposed a new theory by considering the total energy of a ferromagnetic plate system. By including the energy of demagnetization, their theoretical predictions agree with the experimental results of Moon and Pao [20].

In addition to the buckling of soft ferromagnetic plates, deformation and fracture of ferromagnetic materials and ferromagnetic composites constitute another important aspect of magnetoelasticity, attracting much recent attention. Along with the development of giant magnetostrictive alloys of RE and iron, and ferromagnetic shape memory alloys, many researchers have attempted to establish the magnetoelasticity of ferromagnetic materials, including the deformation and fracture of ferromagnetics of large magnetostriction and the effective properties of magnetostrictive composites [12,13]. Since there already exist review articles [35] on the buckling of soft ferromagnetic plates under a magnetic field, we focus in this paper on the recent progress as well as the remaining

Published online March 21, 2008. Transmitted by Assoc. Editor S. Adali.

  

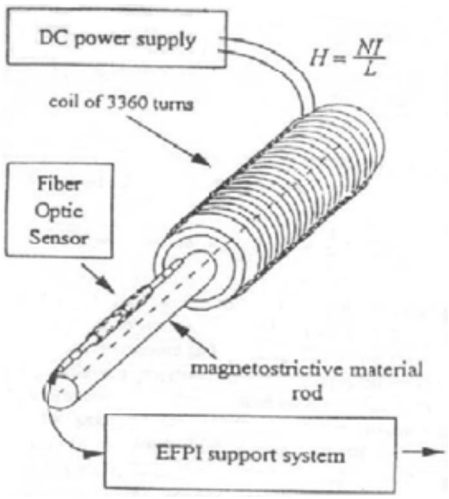


**Fig. 1 Schematic setup of magnetostriction testing with optical fiber [44]**

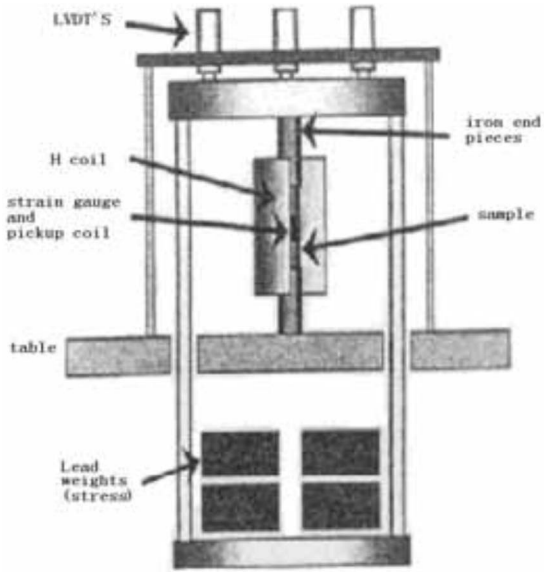


**Fig. 3 Schematic setup of magnetostriction testing with weight loads [45]**

issues regarding the magnetomechanical deformation and fracture of soft ferromagnetic materials from both experimental and theoretical aspects.

## 2 Experiment

**2.1 Magnetomechanical Equipments and Techniques.** With the advance of magnetoelasticity, a multitude of magnetomechanical equipments have been developed. Carman and Mitrovic [44] established a set of equipments to measure the quasistatic magnetostrain (see Fig. 1). This setup measures the longitudinal strain along the direction of the magnetic field by means of an optical fiber attached to the testing sample. The driving magnetic field is generated by a winding coil. The equipment can measure magnetostriction with the accuracy of the order micrometer without obvious disturbance from the external magnetic field. However, this equipment cannot apply mechanical forces to the sample and cannot yet test dynamic magnetostriction.

The Bitter coils can provide a very large magnetic field (see Fig. 2). The components indicated in this figure are the following (1) ferromagnetic composite sample, (2) base, (3) movable capacitor plate, (4) cover, (5) insulator, (6) immovable capacitor plate, (7) distance rod, (8) nut, (9 and 10) leads connecting capacitor plates to a measuring bridge, and (11) winding of Bitter's magnet.

Bednarek [13] employed the Bitter coils to measure the strain of a Terfenol-D particulate composite sample, with the biggest magnetic field reaching 8 T. The magnetostrain is estimated by calculating the change of capacitance between movable and unmovable plates, where the movable plate is attached to the free end of the sample. The limitation of Bitter coils is that there is no device applying mechanical force, and, generally speaking, it is too expensive for a regular measurement.

Figure 3 is a relatively simple magnetomechanical equipment [45] that generates a magnetic field by coils and provides mechanical force by means of adding weights. The test can be conducted under a constant stress in the process of magnetization. However, this equipment cannot provide a large magnetic field, and a large compressive stress is generally not available.

Figure 4 [46] is a magnetostriction-testing equipment having a close magnetic circuit, with silicon sheet as the magnetic-field

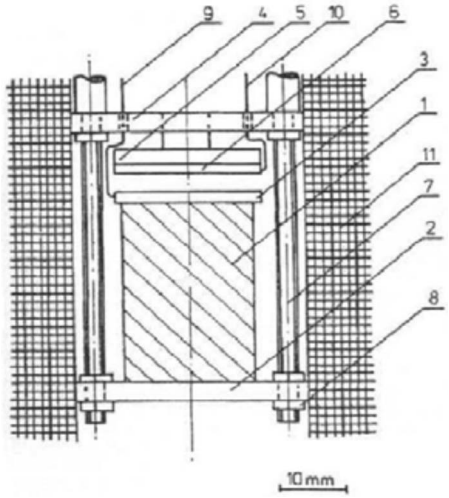


**Fig. 2 Schematic setup of magnetostriction testing with Bitter coils [13]**

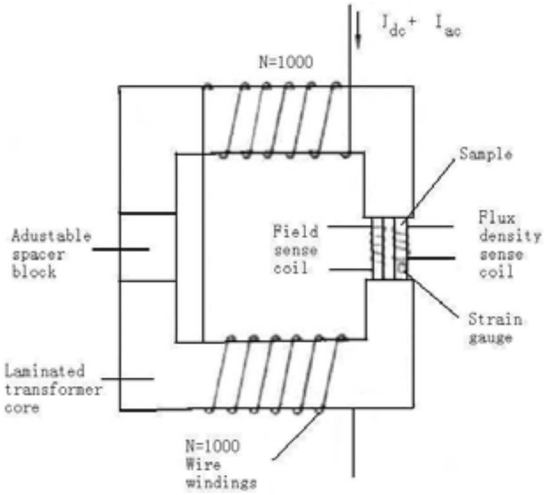


**Fig. 4 Magnetostriction measurement setup with a closed magnetic circuit [46]**

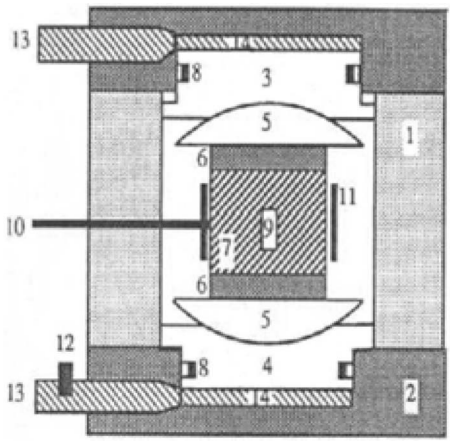


**Fig. 5 Sectional view of a cylindrical sample holder for rods of highly magnetostrictive materials [47]**

conducting medium. An adjustable spacer block is specially designed to ensure that the magnetic circuit remains closed even when the sample, driven by a magnetic field, elongates or contracts. Like all aforementioned testing setups, the magnetic field is produced by a coil. This equipment, however, is rather complex and also lacks components providing mechanical forces.

Figure 5 [47] is a magnetomechanical setup that can offer hydraulic pressure to a testing sample. The cylindrical sample holder for rods of highly magnetostrictive materials can test the sample deformation under a constant prestress. The individual components are as follows: (1) nonmagnetic shell, (2) lid, (3) movable blank plug, (4) unmovable blank plug, (5) spherical support, (6) gasket, (7) sample, (8) sealing strip, (9) stain gauge, (10) Hall probe, (11) coils, (12) pressure transducer, (13) oil circuit for hydraulic pressure, and (14) oil. The magnetostrictive sample can be adjusted to be in pure compression by means of the hydraulic system and the spherical bearing. Magnetic field is produced by an electromagnet. This setup can provide variable magnetic and mechanical loads. The limitation is that only compressive force can be applied. Other kinds of mechanical loads such as tensile and bending forces cannot be exerted.

Figure 6 [48] is the schematic of an experimental arrangement for testing magnetostrictive materials. A water-cooled electromagnet was particularly designed to have one pole piece modified to provide a compressive prestress to the magnetostrictive rod sample. The piston contained in the pole is actuated hydraulically by a hand pump. The largest compressive stress can be 74 MPa. The extensional strain was measured with strain gauges. Variable and constant compressive stresses can be obtained in the process of testing. However, this setup still cannot exert tensile stress to the sample.

To study the deformation and fracture of functional ferromagnetics, the magnetomechanical setup should include devices that can provide both magnetic field and mechanical loads, and also a measurement system for mechanical and magnetic data. The magnetic field is generally provided by an electromagnet or a permanent magnet. Superconducting coil [18,49] can carry intense electric current and produce substantially stronger magnetic field. However, it works typically under a cryogenic environment, requiring a set of supplementary facilities that are usually expensive. On the other hand, the operating space of a superconducting coil is very limited for the mechanical components. Therefore, electromagnet is commonly adopted as the magnetic-field generating equipment.

With the aforementioned objectives in mind, the authors of this paper developed one type of magnetomechanical setup [50,51], as shown in Fig. 7. The entire equipment includes four main parts: electromagnet, mechanical system, measurement system, and con-

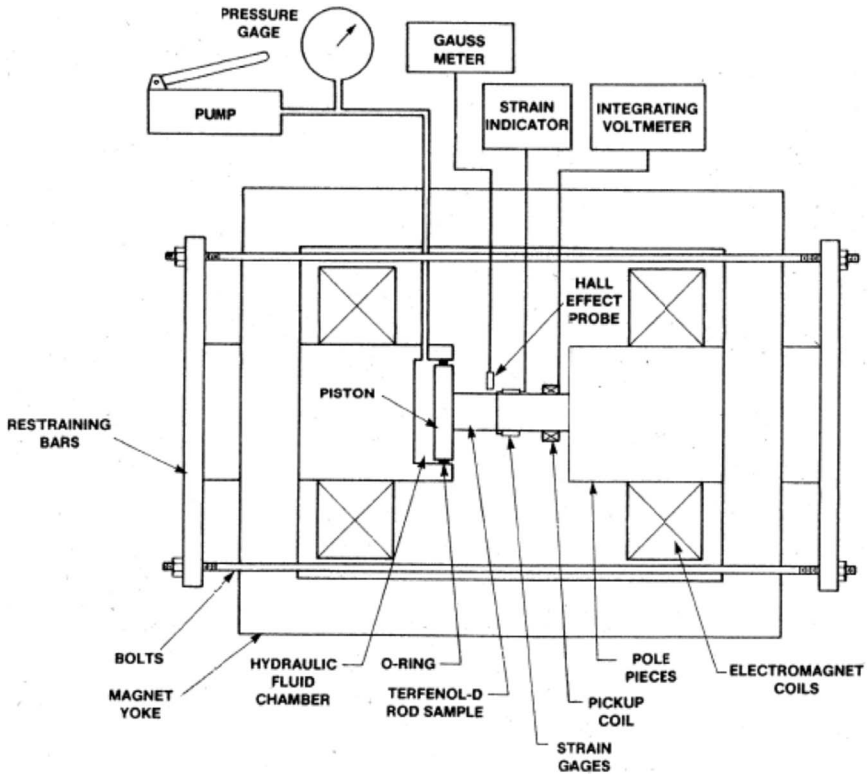


**Fig. 6 Schematic of the experimental setup for magnetostrictive materials with a water-cooled electromagnet [48]**

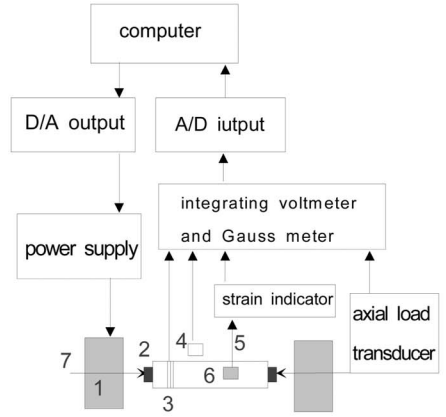


(*a*)

(*b*)

**Fig. 7 (*a*) Schematic and (*b*) photo of experimental setup for coupled magnetomechanical loads [50,51]**

trol and feedback system. The electromagnet can provide a continuously varying magnetic field by changing the intensity of the electric current. This part is equipped with power supply of high stability and wide range applicability. By means of a servoactuator, the mechanical part can provide tensile, compressive, bending, and other loads. Mechanical components for three-point bending and indentation loading are specially considered and designed. The measurement system collects and records the magnetic and mechanical data. The control and feedback system automatically controls and monitors the loading process of the magnetic field as well as the mechanical force. The equipment contains additional hardware (e.g., Gauss meter, Hall probe, mechanical transducer, strain gauge, and integrating instrument) and software (for data collecting, process monitoring, and controlling). To minimize the electromagnetic interference, those parts directly exposed to the magnetic field are specially designed to be made of copper or nonmagnetic stainless steel, and shielded wires are employed for data collecting.

### 2.2 Magnetomechanical Deformation

.

*2.2.1 Soft Ferromagnetic Metals*. The variability of magnetic properties of metals during deformation has been extensively studied for the application of nondestructive evaluation (NDE). It has been established that some soft ferromagnetic metals, such as iron, nickel, and steel, exhibit obvious changes in magnetic properties after deformation, especially after plastic deformation. Cullity [52] found that the magnetization of mild carbon steel increases if a tensile stress is applied in the direction of the magnetic field, and decreases for a compressive stress. Makar and Tanner [53,54] measured the magnetic parameters in an alloy steel under a uniaxial load, with the stress exceeding the yield strength. By studying the stress-induced changes in a coercive field, remanent magnetization, and reversible and total relative differential permeability, they found that the permeability and remanent magnetization can be used to detect the onset of dislocation growth, hence raising the prospect of using a magnetic NDE method to predict failure inner materials. In addition, they also studied the effect of residual stresses on the magnetic properties of an alloy steel.

Stevens [55] studied the magnetic properties of two grades of steel under a uniaxial load within the range of elasticity and found that the magnetic parameters are more sensitive to compressive stress than tensile stress. Takahashi et al. [56] measured the changes in magnetic properties of single-crystal pure iron, polycrystalline iron, and alloy steel under a uniaxial stress that is increased beyond the yield point. Magnetic parameters such as the coercive field and permeability were obtained by measuring the hysteresis loop. It is found the coercive field increases with the applied stress. Within a certain range of the magnetic coercive field, there exists a relation between susceptibility $\chi_c$ and the magnetic field $H$, i.e., $\chi_c = c/H^3$, where $c$ is a material constant that is dependent on crystal defects (e.g., dislocation density) and grain boundary size, but independent of the deformation process and sample. This result is useful in a nondestructive testing for metal fatigue.

Devine and Jiles [57] studied annealed nickel and cobalt with a percentage purity of 99.99%. It is found that the external stress has negligibly small effect on the magnetostriction of cobalt, but has significant impact on nickel. Tensile stress increases magnetostriction, while compressive stress decreases it. The authors of this paper also tested the magnetostriction of nickel [51], with a saturated magnetostriction of −36 ppm at zero stress, rising gradually to −48 ppm at a tensile stress of 318.3 MPa (see Fig. 8(*a*)) while reducing to −22 ppm at a compressive stress of 89.1 MPa (Fig. 8(*b*)).

Pearson et al. [58] measured the magnetomechanical properties of pure iron under biaxial stresses and obtained the relation between the change of coercive field and stress-induced irreversible magnetization, and also the external biaxial stresses. It was found that the change of coercive field is unsymmetrical under biaxial stresses.

*2.2.2 Giant Magnetostrictive Materials of a Rare Earth Alloy*. In 1972, Clark et al. [59,60], for the first time, found that the Laves phase of magnetostrictive alloy of RE element and iron, $RFe_2$ (here, $R$ stands for the RE element such as Tb, Dy, Ho, Er, Sm, and Tm), has the so-called giant magnetostriction at room temperature. Savage et al. [61] later discovered that a RE magnetostrictive alloy is sensitive to prestress. The saturated magnetostriction increases evidently if a prestress is applied on the material. Typically, a RE magnetostrictive alloy has a magnetostrain of the order of $10^{-3}$. In the meantime, this kind of material is quick in response to an external magnetic field, and has a high energy density. Therefore, the RE alloy is usually employed in devices of energy transformation.

There are many reports in literature on the characterization of RE alloys and the exploration of their potential use in practical engineering. Moffet et al. [48] studied in detail the magnetomechanical behavior of Terfenol-D under different prestresses. It was found that a bigger magnetic field is needed to drive the Terfenol-D rod to the same extensional strain as the prestress increases, and the apparent permeability of the material decreases at the same time. Jiles and Thoelke [62] focused on the effect of

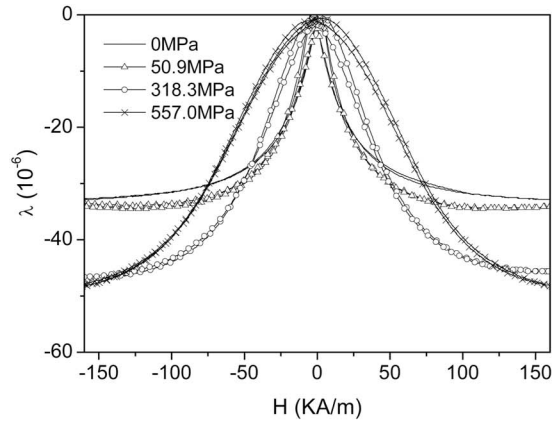


(*a*)

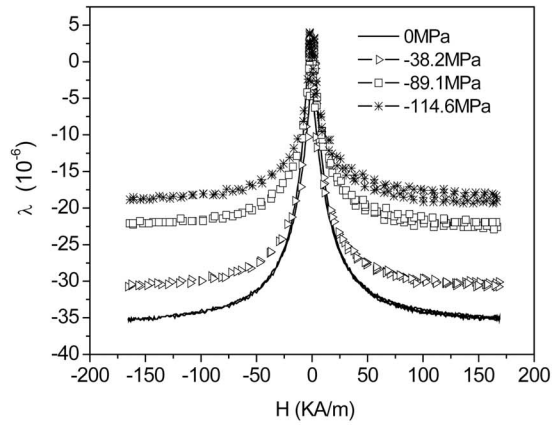


(*b*)

**Fig. 8 Magnetostriction of $Ni_6$ subjected to (*a*) tensile stress and (*b*) compressive stress [51]**

prestresses on the variation of the magnetic behavior of a TbDyFe alloy with different compositions. Furthermore, they gave an explanation in terms of the magnetic domain theory. Mei et al. [63] studied single-crystal TbDyFe with different crystal orientations. They found that magnetostriction in the [110] direction is superior to that along [112]. The best is nonetheless along orientation [111], with a saturated magnetostriction of 1700 ppm under the saturated magnetic field of 500 Oe. Prajapati et al. [64,65] studied the effect of cyclic stress on Terfenol-D and found that stress can enhance magnetocrystalline anisotropy (see Fig. 9), where the dashed and solid lines represent separately the hysteresis loop with and without cycled stress. It can be seen that there is an obvious change in the magnetization loop after cycling.

We [50,51,66] systematically studied the magnetoelastic behavior of polycrystalline TbDyFe under a wide range of prestresses, with the peak stress attaining 80 MPa. The polycrystalline TbDyFe is directed along [110], and the cylindrical sample has a diameter of 10 mm and a length of 30 mm. As shown in Figs. 10 and 11, the magnetostrain grows slowly as the prestress is increased, with the magnetization curve eventually approaching a straight line, as is the general case for paramagnetic materials. Figures 12–15 present experimental results on magnetization curves and stress versus strain relations under different prestresses. It is evident from these results that there exists nonlinearity in magnetization and stress-strain relations. There also exist residual magnetostrain and magnetization.

*2.2.3 Ferromagnetic Shape Memory Alloy*. With giant magnetostriction as well as shape memory effect under a magnetic field,

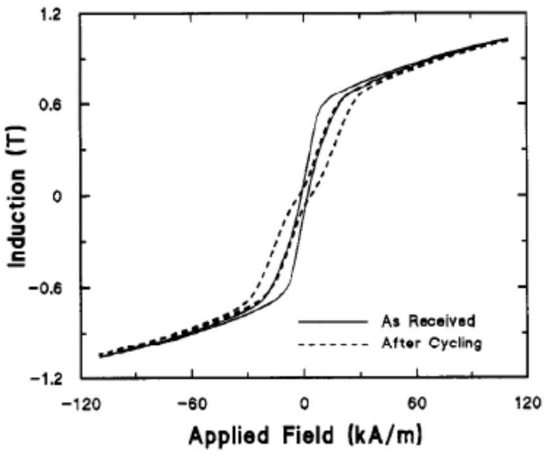


**Fig. 9 Effect of stress cycling on magnetization [64]**

ferromagnetic shape memory alloy NiMnGa is suitable for the new generation of devices [14,15]. The giant magnetostrain of NiMnGa originates from the martensitic phase transformation induced by an external magnetic field. Recent studies show that the

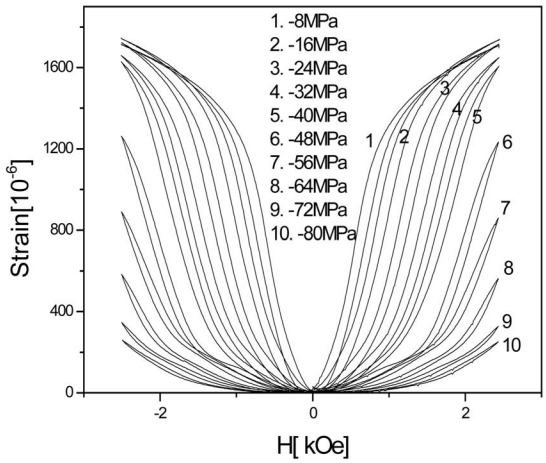


**Fig. 10 Effect of prestress on magnetostriction [50]**

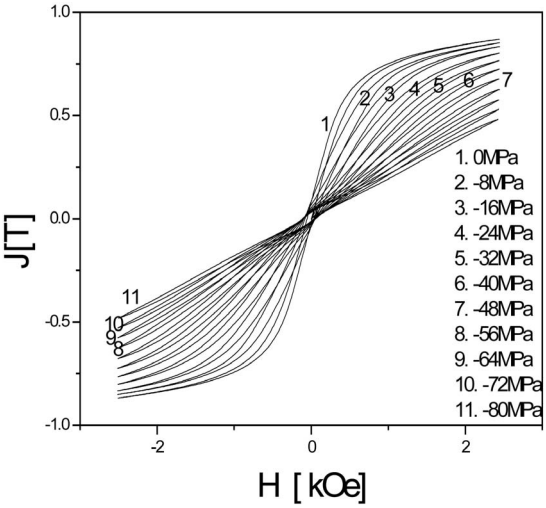


**Fig. 11 Variation of magnetization with prestresses [50]**

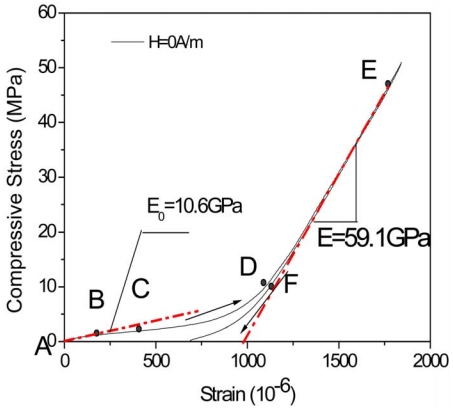


**Fig. 12 Stress plotted as a function of strain without magnetic field [67]**

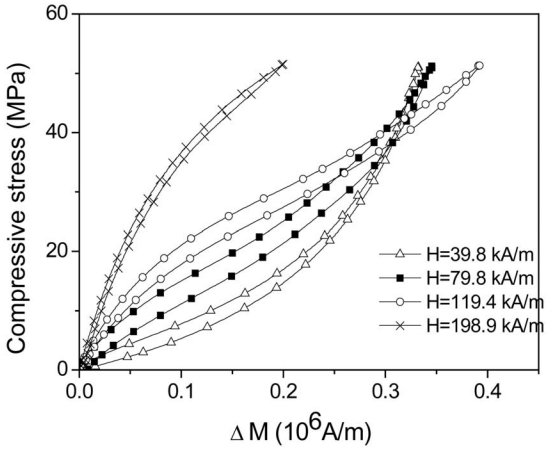


**Fig. 15 Effect of magnetic field stress versus magnetization curve [51]**

magnetostrain of single-crystal NiMnGa can reach a level as large as 9.5% [16]. Wu et al. [17] examined further the cryogenic magnetostriction [18] of this kind of material. There are also recent interests in NiMnGa thin films. For example, Dubowik et al. [67] studied the ferromagnetic resonance of polycrystalline NiMnGa thin films, while Dong et al. [68] investigated the ferromagnetic shape memory effect of single-crystalline NiMnGa thin films.

We [69] studied the magnetoelastic behavior of the alloy of NiMnGa and Fe at room temperature. The sample used is the $Ni_{52}Mn_{16}Fe_8Ga_{24}$ single crystal, with [001] being the growing direction. Its martensitic phase temperature $M_s$, austenitic temperature $A_s$, and Curie temperature $T_C$ are 262 K, 286 K, and 381 K, respectively. At room temperature, the sample is in the state of parent phase, i.e., austenite. Figures 16 and 17 display the magnetostriction curves associated with different prestress levels. In Fig. 16, the stress is parallel to the magnetic field, while in Fig. 17, the stress is perpendicular to the magnetic field.

As for the mechanism of the effect of magnetic field on the transformation of NiMnGa, Liang et al. [70] employed the bending method of small sample strips to study transformation-induced deformation in magnetic fields. They noticed that the direct magnetic effects on martensitic transformations were small. While the stress-induced transformations are appreciable in this kind of materials due to the magnetic forces that originated from the magnetic-field gradient. They also concluded that a careful examination of the magnetic force caused by nonuniformity of the magnetic field should be taken for the purpose of addressing the role of magnetic field in transformation. Jeong et al. [71] studied the effect of magnetic field on the transformation start temperature. The results showed that the martensite-start temperature ($M_S$) increases with an increase of magnetic field. The linear relationship between the magnetic field and the $M_S$ was confirmed in terms of the experimental results and the modified Clausius–Clapeyron equation.

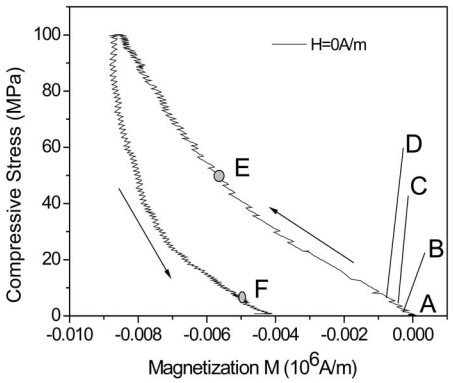


**Fig. 13 Stress versus magnetization curve without magnetic field [67]**

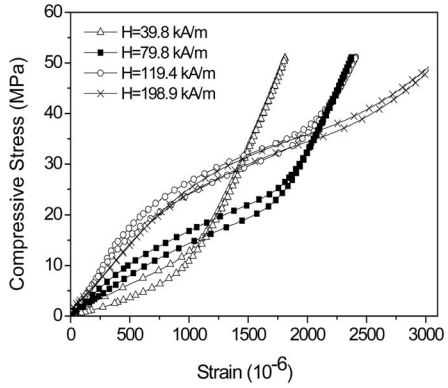


**Fig. 14 Strain versus stress curve in the presence of magnetic field [51]**

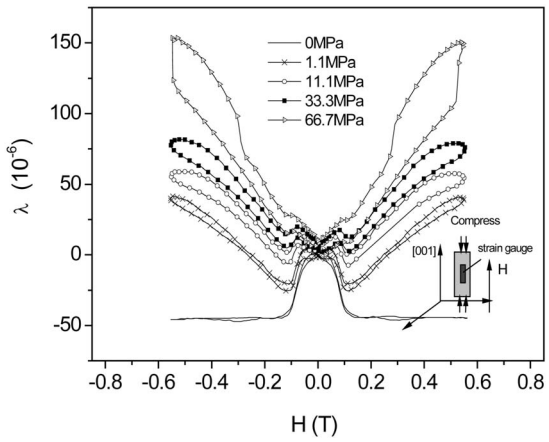


**Fig. 16 Magnetostriction of single-crystal $Ni_{52}Mn_{16}Fe_8Ga_{24}$ [69]**

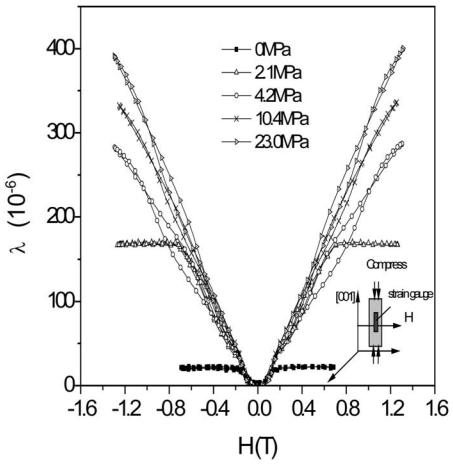


**Fig. 17 Magnetostriction of single-crystal $Ni_{52}Mn_{16}Fe_8Ga_{24}$ [69]**

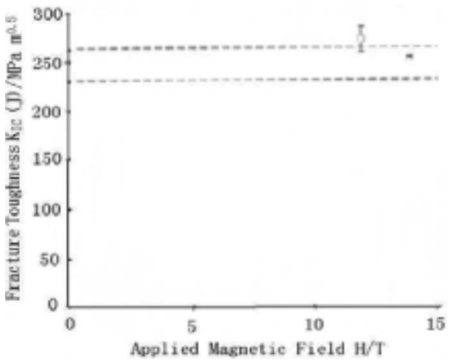


**Fig. 19 Fracture toughness of Incoloy908 under various magnetic fields [49]**

**2.3 Magnetomechanical Fracture.** The widespread applications of magnetic materials in engineering have raised the concern for their reliability under a strong external magnetic field. Since flaws such as cracks, voids, and inhomogeneities inevitably exist in materials, the fracture of magnetic materials has become an important subject.

Clatterbuck et al. [49] measured the fracture toughness of Incoloy908, a soft ferromagnetic alloy, using the compact tension (CT) specimen under cryogenic conditions, where the peak magnetic field reached 14 T. Figure 18 displays the fracture resistance curves of Incoloy908 under various magnetic fields (0 T, 12 T, and 14 T), while Fig. 19 plots its fracture toughness in which the dashed lines indicate the scattering of experimental data. These results reveal that there is no obvious effect of external magnetic field on the fracture toughness of the alloy.

To evaluate the magnetic effect on fracture properties of the ferromagnetic austenitic alloy 908, the small specimen testing techniques [72], such as the notch tensile and small punch tests, are employed in cryogenic high magnetic-field environments. Results show that the 4 K fracture properties of alloy 908 are not changed significantly by magnetic fields. The experimental results are in agreement with the theoretical model that predicts a negligible magnetic-field effect on the stress intensity factor (SIF) for a crack in low-permeability materials.

We [73] measured the fracture toughness of manganese-zinc ferrite ceramics with different permeabilities (2000 and 10,000) by means of the three-point-bending method under external magnetic field. Single-edge-notch-beam (SENB) specimens with dimensions of $3\times4.8\times30$ mm$^3$ and with a notch of $0.2\times0.6\times3$ mm$^3$ on each side of the specimen were used. For the two groups of samples with different specific magnetic permeabilities, Fig. 20 shows that the average fracture toughness is 1.37 MPa $\sqrt{\text{m}}$ and 1.38 MPa $\sqrt{\text{m}}$, respectively. There is no measurable change of fracture toughness by varying either the magnetic field or the specific magnetic permeability.

In addition to the three-point-bending test, we [73] also adopted Vickers' indentation technique under a magnetic field to study the fracture behavior of manganese-zinc ferrite ceramics with different specific magnetic permeabilities. The specimens have the dimensions of $3\times10\times30$ mm$^3$. One $10\times30$ mm$^2$ surface was grounded and polished to a mirror finish with diamond pastes. The average indentation load is 50 N. The measured average diagonal length of the pyramid indent is 107 $\mu$m and the average Vickers hardness of the samples is 8 GPa. Table 1 lists the indentation results, where $C_{\parallel}$ and $C_{\perp}$ are, respectively, the crack length along the direction parallel to the magnetic field and the direction perpendicular to the magnetic field. There is no visible change in the apparent fracture toughness of the samples under various external magnetic fields, and also no obvious fracture anisotropy was observed.

The above experimental results show that the external magnetic field has no visible influence on the fracture toughness of ferromagnetic materials tested. However, some others reported a significant magnetic effect on fracture parameters such as the SIFs. Shindo et al. [74] selected three kinds of soft magnetic materials

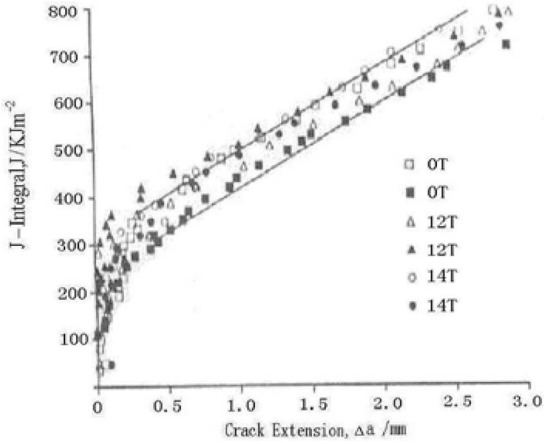


**Fig. 18 Fracture resistance curve of Incoloy908 under various magnetic fields [49]**

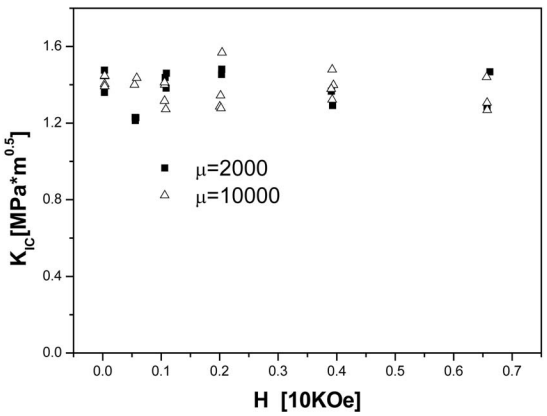


**Fig. 20 Effect of relative permeability and magnetic field on fracture toughness of manganese-zinc ferrite ceramic [73]**

**Table 1 Experimental results with Vickers' indentation[73]**

| Relative permeability | Parallel to the magnetic field | | Perpendicular to the magnetic field | |
|---|---|---|---|---|
| | $K_{IC}$ (MPa $\sqrt{m}$) | $C_{\parallel}$ ($\mu$m) | $K_{IC}$ (MPa $\sqrt{m}$) | $C_{\perp}$ ($\mu$m) |
| 2000 | 0.92 | 228 | 0.93 | 226 |
| 5000 | 1.04 | 210 | 1.03 | 212 |
| 10,000 | 1.03 | 212 | 1.02 | 213 |

with different specific magnetic permeabilities, i.e., TMC-V: $\mu_r$ =27,900; TMH-B: $\mu_r$=10,690, and TMB: $\mu_r$=9030, respectively, as the candidate materials. The specimen plates were 140 mm long and 1 mm thick, and 40 mm wide, with a center-through crack of different lengths. A tensile load and a static uniform magnetic field of magnetic induction $B_0$ normal to the crack surface were simultaneously applied. The strain gauge method was used to determine the magnetic SIF. The results are shown in Fig. 21, where $h$ and $a$ are, respectively, half of the strip width and crack length. $b_c$ is a dimensionless quantity indicating the magnetic field of magnetic induction $B_0$ applied at infinity, $k_{h1}$ is the SIF with magnetic effect, and $\sigma_0$ is the uniform normal stress applied at infinity. It can be seen that the SIF increases in the presence of an external magnetic field, and the magnetic-field effect is more pronounced for the materials with a larger specific magnetic permeability.

Furthermore, the magnetic-field effect was experimentally studied on the soft ferromagnetic plate with a thickness-through crack under the dual action of a uniform transverse magnetic field and a normal line load [75]. Ferritic stainless-steel SUS430 was used as a specimen material ($\mu_r$=122.9). Three kinds of specimens were used, i.e., the specimen with single-internal crack, single-edge crack, and two symmetric edge cracks, respectively. Strain gauges were used to evaluate the magnetic-moment intensity factors. See Figs. 22–24 for the results, where $l$ and $W$ are the length and width of the specimen, respectively. $h$ and $a$ are half of the thickness and crack length. $P$ is the mechanical load. The vertical axis shows the moment intensity factor with magnetic effect, $K_1$, normalized by that produced by pure mechanical load, $K_{10}$. It can be seen that the moment intensity factor increases with an increasing magnetic field. There is no dependence of the moment intensity factor with magnetic field on the load.

In addition to the magnetic effect on the static fracture parameters, Shindo et al. [76] also further explored on the dynamic magnetoelastic fracture problem. Magnetic effect on the crack growth rate (CGR) was investigated by means of the single-edge cracked plate specimen of a nickel-iron soft magnetic alloy under a uniform magnetic field normal to the crack face. A through-the-thickness notch was first machined and then fatigue precracked. The crack opening displacement was measured by a clip gauge. Shown in Fig. 25 is the normalized CGR with magnetic effect versus the normalized magnetic field, in which CGR0 is the CGR

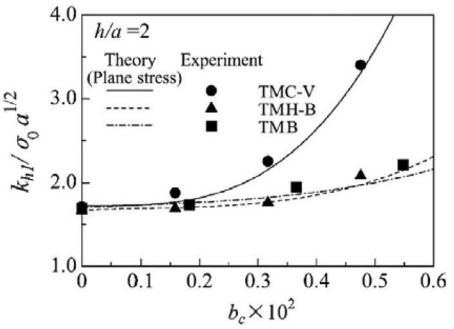


**Fig. 21 SIF versus magnetic field [74]**

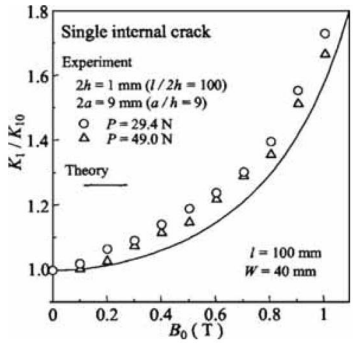


**Fig. 22 Comparison of the measured magnetic-moment intensity factor with the theoretical result (single-internal crack) [75]**

without a magnetic field and $a/h$ is the ratio of original crack length to the width of a single-edge cracked strip. It can be found that the CGR increases with external magnetic field. Cracks will grow fast with the aid of an external magnetic field. From the experimental data, there seems to be a linear relation between the CGR and the magnetic field, though the authors predicted a nonlinear relation by their theoretical model.

Obviously, experiments in the open literature give two kinds of completely different results with regard to the magnetic effect on fracture parameters. Some experiments showed no measurable effect [49,72,73], while some others found a significant effect [74–76]. In the experiments where the magnetic field are perpendicular to the crack surface and parallel to the wide face, such as the experiments with the CT specimen, the fracture toughness was

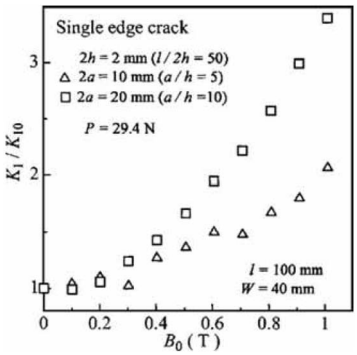


**Fig. 23 Moment intensity factor versus magnetic field (single-edge crack) [75]**

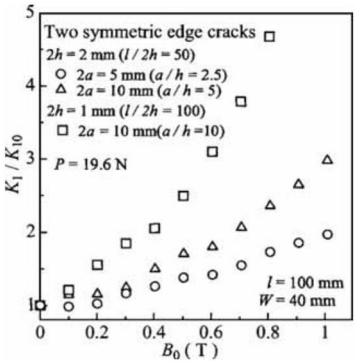


**Fig. 24 Moment intensity factor versus magnetic field (two symmetric-edge cracks) [75]**

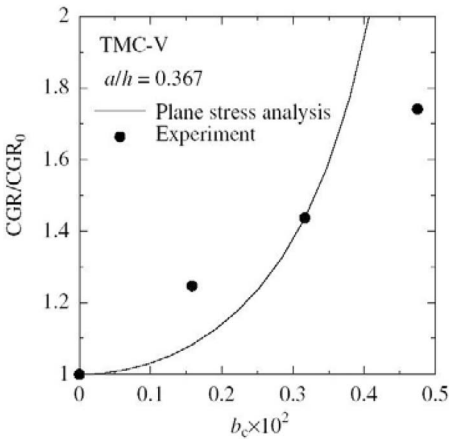


**Fig. 25 CGR versus magnetic field [76]**

not affected by even a very high magnetic field. However, for the bending plate with a through-thickness crack under a transverse magnetic field and a normal mechanical load, the magnetic effect can be significant. Judged by the experiments and their theoretical analysis, Horiguchi and Shindo [75] concluded that the magnetic-field effect on fracture mechanics parameters depends on the direction of magnetic field and mechanical loading condition.

## 3 Nonlinear Constitutive Relations

**3.1 Phenomenological Constitutive Relations Based on Thermodynamics.** The interaction of magnetic field and the elastically deformable solids has been theoretically studied within the framework of phenomenological thermodynamics several decades ago. By means of the general principle of continuum mechanics, Maugin and Eringen [77,78] derived the coupling constitutive theory from the viewpoint of magnetomechanical interaction and the quantum interchange origin of magnetic field. This theory is nonetheless rather complicated for a magnetomechanical analysis. Pao [3] and Pao and Yeh [24] focused on soft ferromagnetic materials of multidomains, where the magnetic hysteresis loss and the interchange effect of quantum can be neglected. The constitutive equations are as follows:

$$t_{ij} = \rho \frac{\partial x_i}{\partial X_K} \frac{\partial U}{\partial E_{KL}} \frac{\partial x_j}{\partial X_L} + M_j \frac{\partial U}{\partial N_K} \frac{\partial x_j}{\partial X_K} \tag{3.1}$$

$$\mu_0 H_i = \frac{\partial U}{\partial N_K} \frac{\partial x_i}{\partial X_K} \tag{3.2}$$

where $t_{ij}$ is the magnetoelastic stress tensor, $U=U(E_{IJ},N_J)$ the internal energy density, $\rho$ the mass density, $M_i$ the magnetization vector, $H_i$ the magnetic-field vector, and $\mu_0$ the vacuum permeability. $x_i$ and $X_J$ are position vectors in the configurations prior to and after deformation,

$$N_J = \frac{M_k}{\rho} \frac{\partial x_k}{\partial X_J} \tag{3.3}$$

The magnetoelastic constitutive relations given by Eqs. (3.1) and (3.2) were further linearized on the basis of small deformation [24]. According to the perturbation method, all magnetoelastic quantities can be divided into two parts, one in the rigid state and the other relevant to deformation. Furthermore, higher order quantities can be ignored due to the small deformation assumption. Consequently, the governing field equations, constitutive equations, and boundary conditions can all be simplified. This linearized version of constitutive theory has received much attention due to its simplicity and physical soundness. On the other hand, Jiles and Atherton [79,80] and Jiles [81] proposed one phenomenological model based on the experimental hysteresis loop; the coefficients in this model are obtained by fitting with experimental data using the least squares method.

The giant magnetostrictive alloy of RE and iron belongs to the soft ferromagnetic materials, which possesses very large magnetostrain, high energy density, and relatively narrow hysteresis loop. Carman and Mitrovic [44] developed constitutive relations by truncating the Taylor series of the Gibbs free energy; the one-dimensional form of these relations can be obtained with reference to experimental results. The pseudolinear version of the magnetostrictive constitutive relations can be arranged around a biased magnetic field, as follows:

$$\varepsilon_{ij} = s'_{ijkl}\sigma_{kl} + d'_{nij}H_n + \alpha'_{ij}\Delta T$$

$$B_n = \mu'_{ni}H_i + d'_{nij}\sigma_{ij} + P'_n\Delta T \tag{3.4}$$

where $s'_{ijkl}$, $d'_{nij}$, $\alpha'_{ij}$, $\mu'_{nil}$, and $P'_n$ are compliance, piezomagnetic coefficients, thermal coefficient, magnetic permeability, and thermomagnetic coefficients, all being functions of the bias magnetic field. In general, it is difficult to quantitatively define these coefficients since they are not real material constants. To overcome this difficulty, the authors of this paper [82–84] have reexamined the constitutive behavior of the giant magnetostrictive rod. A new method was proposed to determine the above constitutive coefficients. Furthermore, a new constitutive model, i.e., the density of the domain switching model, was developed.

*3.1.1 Standard Square Model [82–84].* Experimental results have shown that the magnetostrain of magnetostrictive materials generally varies nonlinearly with the applied magnetic field. When the magnetic field becomes very large, the magnetostrain saturates. It was also revealed that the magnetostrain remains unchanged when magnetic field changes to its opposite direction with the same magnitude, suggesting that magnetostrain is an even function of magnetic field. Consequently, the one-dimensional constitutive equations may be phenomenologically established as

$$\varepsilon = s\sigma + mH^2 + r\sigma H^2, \quad B = \mu H + 2m\sigma H + r\sigma^2 H \tag{3.5}$$

where $s$ is the elastic compliance, $m$ the magnetostrictive modulus, $r$ the magnetoelastic coefficient, $\mu$ the permeability, $\varepsilon$ the strain, $\sigma$ the stress, $H$ the magnetic field, and $B$ the magnetic induction. The coefficients are determined as

$$m = \frac{\tilde{d}_0}{s\tilde{H}_0}, \quad = \frac{1}{\sigma}\left[\frac{\tilde{d}_{\rm cr} + a\cdot\Delta\sigma + b\cdot(\Delta\sigma)^2}{2(\tilde{H}_{\rm cr} + \zeta\cdot\Delta\sigma)} - \frac{\tilde{d}_0}{2\tilde{H}_0}\right] \tag{3.6}$$

where the piezomagnetic coefficient can be expressed as

$$\tilde{d} = \tilde{d}_{\rm cr} + a\cdot\Delta\sigma + b\cdot(\Delta\sigma)^2 \tag{3.7}$$

Here, $\tilde{d}_0$ is the maximum piezomagnetic coefficient, $\tilde{H}_0$ is the external magnetic field associated with the maximum piezomagnetic coefficient in the absence of compressive prestress, while $\tilde{d}_{\rm cr}$ and $\tilde{H}_{\rm cr}$ are the values corresponding to the case of critical compressive prestress. The coefficients $a$ and $b$ can be determined in terms of experimental data. For the giant magnetostrictive alloy of RE and iron, the piezomagnetic coefficients are generally not constant, varying with the bias conditions such as the compressive prestress and the magnetic field, as illustrated in Fig. 26.

The driving external magnetic field $\tilde{H}$, associated with the maximum piezomagnetic coefficient $\tilde{d}$ and denoted by the star symbol in Fig. 26, increases as the compressive prestress increases. As schematically demonstrated in Fig. 27, the dependence of the driving external magnetic field $\tilde{H}$ on compressive stress can be approximately fitted by a linear equation as

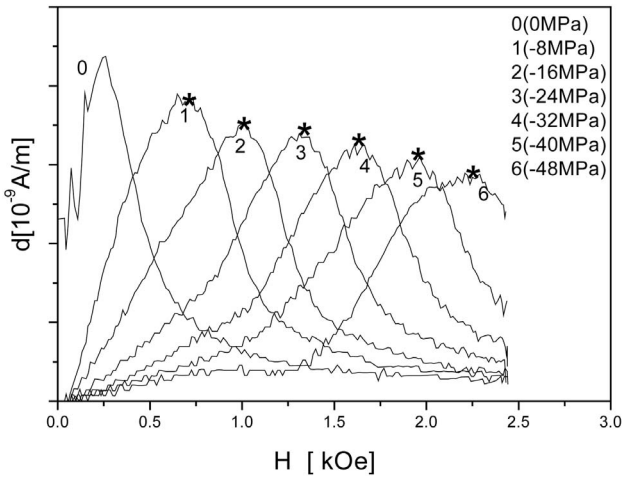


**Fig. 26 Experimental curves of magnetic field (*H*) dependence of piezomagnetic coefficient (*d*) [84]**

$$\tilde{H} = \tilde{H}_{cr} + \zeta \cdot \Delta\sigma \tag{3.8}$$

where $\Delta\sigma = \sigma - \sigma_{cr}$ and $\sigma_{cr}$ is the critical compressive stress for magnetostrictive materials, and $\zeta$ is a material constant with the dimension $A\,m\,N^{-1}$ and physically denotes the increase of the external magnetic field to reach the peak piezomagnetic coefficient due to the increase of external stress.

*3.1.2 Hyperbolic Tangent Constitutive Model*. The hyperbolic tangent model can be obtained by including the hyperbolic tangent function in the thermodynamic Gibbs free energy function, resulting in

$$\varepsilon = s\sigma + \frac{1}{k^2} m \tanh^2(kH) + \frac{1}{k^2} r\sigma \tanh^2(kH) \tag{3.9}$$

$$B = \mu H + \frac{2}{k} m\sigma \frac{\sinh(kH)}{\cosh^3(kH)} + \frac{1}{k} r\sigma^2 \frac{\sinh(kH)}{\cosh^3(kH)} \tag{3.10}$$

where $k = 1/\tilde{H}$ and

$$m = \frac{1}{\tanh(1)(1 - \tanh^2(1))} \frac{\tilde{d}_0}{2\tilde{H}_0} \tag{3.11}$$

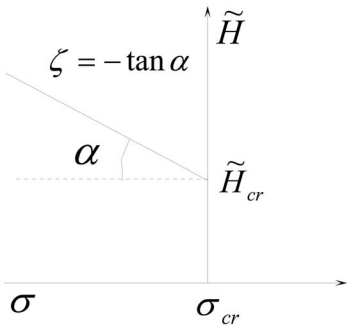


**Fig. 27 Schematic of compressive stress dependence of $\tilde{H}$ [84]**

$$r = \frac{1}{2\tanh(1)(1 - \tanh^2(1))} \frac{1}{\sigma} \left[ \frac{d_{cr} + a \cdot \Delta\sigma + b \cdot (\Delta\sigma)^2}{\tilde{H}_{cr} + \zeta \cdot \Delta\sigma} - \frac{\tilde{d}_0}{2\tilde{H}_0} \right] \tag{3.12}$$

The material parameters $\tilde{d}_0$, $\tilde{d}_{cr}$, $\tilde{H}_0$, $\tilde{H}_{cr}$, $a$, $b$, and $\zeta$ have already been described in the preceding sections and can be determined by controlled experiments.

*3.1.3 Constitutive Relations Based on the Density of Domain Switching [83]*. This constitutive model was proposed by adopting the phenomenological description of domain switching in magnetic materials. A large quantity of magnetic domains exists in magnetic materials, which will turn to the direction of external magnetic field, resulting in magnetostriction. If the density of domain switching is defined by the quantity of domain switching induced by a unit magnetic field, then macroscopically this definition can be viewed as the deformation caused by the unit external magnetic field.

The density of domain switching can be approximately simulated by the normal distribution of a probability density function. The one-dimensional version of the constitutive relations can then be expressed as

$$\begin{aligned} \varepsilon = {} & s \cdot \sigma + \frac{\sqrt{\pi}}{2} \cdot [\tilde{H}_{cr} + \zeta \cdot (\sigma - \sigma_{cr})] \\ & \cdot [\tilde{d}_{cr} + a \cdot (\sigma - \sigma_{cr}) + b \cdot (\sigma - \sigma_{cr})^2] \\ & \cdot \sqrt{\frac{\sigma_{cr}}{\sigma}} \left\{ \operatorname{erf}\left[ \sqrt{\frac{\sigma}{\sigma_{cr}}} \left( \frac{|H|}{\tilde{H}_{cr} + \zeta \cdot (\sigma - \sigma_{cr})} - 1 \right) \right] \right. \\ & \left. - \operatorname{erf}\left( - \sqrt{\frac{\sigma}{\sigma_{cr}}} \right) \right\} \end{aligned} \tag{3.13}$$

$$\begin{aligned} B = {} & \mu \cdot H + \operatorname{sgn}(H) \int_0^{\sigma} [\tilde{d}_{cr} + a \cdot (\sigma - \sigma_{cr}) + b \cdot (\sigma - \sigma_{cr})^2] \\ & \times \exp\left[ - \frac{\sigma}{\sigma_{cr}} \left( \frac{|H|}{\tilde{H}_{cr} + \zeta \cdot (\sigma - \sigma_{cr})} - 1 \right)^2 \right] d\sigma \end{aligned} \tag{3.14}$$

where $H$ is the external magnetic field, $\sigma$ is the stress, $\sigma_{cr}$ is the critical stress for magnetic domain switching, erf denotes the error function, and ($s$, $\mu$, $\tilde{H}_{cr}$, $\tilde{d}_{cr}$, $\sigma_{cr}$, and $\zeta$) are material constants.

A unique feature of the above three kinds of constitutive relations is that they all contain the same constitutive parameters, which can be explicitly determined by experimental data. A comparison of experimental results and theoretical predictions indicates that the standard square model accurately simulates the experimental results in the low and medium regimes of external magnetic field, while under an intense magnetic field, it cannot reflect the saturation of magnetostrain. The hyperbolic model can simulate the magnetostrain under low and medium magnetic fields and can reflect the saturation to some extent under a high magnetic field; however, it cannot capture the sensitivity of material response to various prestresses. The domain-switching density model, on the other hand, captures all the characteristics of the giant magnetostrictive rod under dual action of magnetic and mechanical loads and, therefore, can simulate the experimental results quite well.

Intended for modeling the $\Delta E$ effect of the Tb–Dy–Fe series alloy under both tensile and compressive prestresses, a more complicated one-dimensional constitutive model [85] was developed based on the phenomenological description of the experimental results of the TbDyFe alloy and by choosing the stress and magnetization as independent variables, yielding

$$\varepsilon = \frac{\sigma}{E_s} + \begin{cases} \lambda_s \tanh\left(\frac{\sigma}{\sigma_s}\right) + \left(1 - \tanh\left(\frac{\sigma}{\sigma_s}\right)\right)\frac{\lambda_s}{M_s^2}M^2, & \frac{\sigma}{\sigma} \geqslant 0 \\ \frac{\lambda_s}{2}\tanh\left(\frac{2\sigma}{\sigma_s}\right) + \left(1 - \frac{1}{2}\tanh\left(\frac{2\sigma}{\sigma_s}\right)\right)\frac{\lambda_s}{M_s^2}M^2, & \frac{\sigma}{\sigma_s} < 0 \end{cases} \tag{3.15}$$

$$H = \frac{1}{k}f^{-1}\left(\frac{M}{M_s}\right) - \begin{cases} 2\left(\sigma - \sigma_s \ln\cos\left(\frac{\sigma}{\sigma_s}\right)\right)\frac{\lambda_s}{\mu_0 M_s^2}M, & \frac{\sigma}{\sigma} \geqslant 0 \\ 2\left(\sigma - \frac{1}{4}\sigma_s \ln\cos\left(\frac{2\sigma}{\sigma_s}\right)\right)\frac{\lambda_s}{\mu_0 M_s^2}M, & \frac{\sigma}{\sigma_s} \geqslant 0 \end{cases} \tag{3.16}$$

where $f(x)=\coth(x)-1/x$; $\varepsilon$ and $\sigma$ are the strain and stress, $H$ and $M$ are the magnetic field and magnetization, $M_s$ is the saturation magnetization, and $\lambda_s$ is the saturation magnetostriction; $\sigma_s = \lambda_s E_s E_0/(E_s - E_0)$, where $E_s$ is the intrinsic Young modulus and $E_0$ is the initial Young modulus; $k=3\chi_m/M_s$ is the relaxation factor, where $\chi_m$ denotes the linear magnetic susceptibility.

In addition, a nonlinear magnetomechanical coupling model consisting of the modified Rayleigh model for the magnetic polarization and the "butterfly curve" model for the strain was developed [86]. This constitutive model was developed based on the thermodynamic frame with the assumption of a negligibly small change of material internal stress during magnetic polarization and magnetostriction, and expected for predicting the constitutive hysteresis for the giant magnetostrictive thin films on a nonmagnetic substrate at low magnetic fields.

**3.2 Constitutive Model Based on Noncontinuous Domain Switching.** From the microscopic viewpoint of magnetization, magnetostriction is the result of magnetic domain switching. For the widely used giant magnetostrictive alloy, Terfenol-D, the easy axes of magnetization are the [111] crystalline axes. In terms of the minimum free energy principle, magnetic domains must be in the direction of ⟨111⟩, where domain walls intersect each other with angles of 0 deg, 71 deg, and 109 deg, respectively. Verhoeven et al. [87] experimentally studied the single crystal TbDyFe oriented along the [112] direction and found that magnetic domains turn to the direction of $[11\bar{1}]$, which is vertical to the growth orientation of the single crystal, i.e., the crystalline axis [112]. Jiles and Thoelke [88] first proposed a three-dimensional magnetic domain rotation model for single crystals oriented along the [112] direction, supposing that the total free energy is composed of three parts: magnetocrystalline anisotropic energy $E_{\text{ant}}$, external magnetic energy $E_H$, and magnetoelastic energy pertaining to magnetostriction $E_\sigma$, namely,

$$E_{\text{ani}} = E_0 + K_1(\cos^2\theta_1\cos^2\theta_2 + \cos^2\theta_2\cos^2\theta_3 + \cos^2\theta_3\cos^2\theta_1) \tag{3.17}$$

$$E_H = -\mu_0 M_s H(\cos\theta_1\cos\phi_1 + \cos\theta_2\cos\phi_2 + \cos\theta_3\cos\phi_3) \tag{3.18}$$

$$\begin{aligned} E_\sigma = &-\frac{3}{2}\lambda_{100}\sigma(\cos^2\theta_1\cos^2\beta_1 + \cos^2\theta_2\cos^2\beta_2 + \cos^2\theta_3\cos^2\beta_3) \\ &- 3\lambda_{111}\sigma(\cos\theta_1\cos\theta_2\cos\beta_1\cos\beta_2 \\ &+ \cos\theta_2\cos\theta_3\cos\beta_2\cos\beta_3 + \cos\theta_3\cos\theta_1\cos\beta_3\cos\beta_1) \end{aligned} \tag{3.19}$$

where $\cos\theta_i$, $\cos\phi_i$, and $\cos\beta_i$ are the cosine directions of magnetization vector, external magnetic field, and external prestress in the coordinates of crystalline axes, respectively; $E_0$ is the reference energy state; $K_1$ is the crystalline anisotropic coefficients; $\mu_0$ is the permeability of vacuum; $M_s$ is the saturation magnetization; $H$ is the external magnetic field; $\sigma$ is the stress; and $\lambda_{111}$ and $\lambda_{100}$ are the magnetostrictive coefficients in the direction of [111] and [100]. The total free energy of the system can be expressed as

$$E_{\text{total}} = E_{\text{ani}} + E_H + E_\sigma \tag{3.20}$$

The rotation angle of magnetic domain can then be obtained by minimizing the total free energy. Armstrong [89,90] subsequently introduced a probability density function to describe the distribution of magnetic domains based on the model of Jiles and Thoelke [88] and estimated the macroscale magnetostriction and magnetization by means of integral expressions. This model successfully predicts the experimental results of single-crystal TbDyFe oriented toward the [112] direction.

By adopting the assumption of noncontinuous magnetic domain switching, we [51] simulated the constitutive behavior of Terfenol-D. Magnetic domains are supposed to be uniformly distributed in the eight equivalent directions of ⟨111⟩, with the volume fraction of magnetic domain in each direction denoted as $P_i(i=1,\ldots,8)$. It is further assumed that only when the driving force reaches the threshold value can magnetic domains switch to another direction. In this model, the 90 deg domain switching is considered and the so-called 180 deg domain switching is taken as two continuous rotations of 90 deg switching. The stress and magnetic field acting on each domain are supposed to be identical as the external stress and magnetic fields. The free energy for a separate magnetic domain is expressed as

$$G = -\left(\varepsilon_{ij}^*\sigma_{ij} + B_i^* H_i + \frac{1}{2}\sigma_{ij}C_{ijkl}\sigma_{kl} + \frac{1}{2}H_i\mu_{ij}H_j + H_i q_{ikl}\sigma_{kl}\right) \tag{3.21}$$

where $\varepsilon_{ij}^*$ and $B_i^*$ are the eigenstrain and eigenmagnetic induction, $C_{ijkl}$ the elastic compliance, $q_{ijk}$ the piezomagnetic coefficients, $\mu_{ij}$ the permeability, $\sigma_{ij}$ the stress, and $H_j$ the magnetic field. The driving force for the 90 deg domain switching is defined as

$$F_{90}(\theta,\varphi,\psi,\sigma_{ij}^i,H_j^i)\max\{G(\theta,\phi,\varphi;\sigma_{ij}^t,H_j^t,S_t) - G(\theta,\phi,\varphi;\sigma_{ij}^i,H_j^i,S_i)\} \tag{3.22}$$

where $(\theta,\phi,\varphi)$ are the Euler angles of magnetic domain in the global coordinates, $t$ denotes the current state, $i$ represents the possible state after the 90 deg domain switching, $S_i$ is the current type of magnetic domains, and $S_i$ is the possible type of magnetic domains. The macroscopic form of the constitutive equations is

$$\bar{\varepsilon}_{ij} = \bar{\varepsilon}_{ij}^* + \bar{C}_{ijkl}\sigma_{kl} + \bar{q}_{kij}H_k \tag{3.23}$$

$$\bar{B}_i = \bar{B}_i^* + \bar{q}_{ikl}\sigma_{kl} + \bar{\mu}_{ij}H_j \tag{3.24}$$

where

$$\bar{\varepsilon}_{ij}^* = \frac{1}{8\pi^2}\int_0^\pi\int_0^{2\pi}\int_0^{2\pi}\varepsilon_{ij}^*(\theta,\varphi,\psi)\sin\theta\, d\psi d\varphi d\theta \tag{3.25}$$

$$\bar{B}_i^* = \frac{1}{8\pi^2}\int_0^\pi\int_0^{2\pi}\int_0^{2\pi}B_i^*(\theta,\varphi,\psi)\sin\theta\, d\psi d\varphi d\theta \tag{3.26}$$

$$\bar{C}_{ijkl} = \frac{1}{8\pi^2}\int_0^\pi\int_0^{2\pi}\int_0^{2\pi}C_{ijkl}(\theta,\varphi,\psi)\sin\theta\, d\psi d\varphi d\theta \tag{3.27}$$

$$\bar{q}_{ijk} = \frac{1}{8\pi^2}\int_0^\pi\int_0^{2\pi}\int_0^{2\pi}q_{ijk}(\theta,\varphi,\psi)\sin\theta\, d\psi d\varphi d\theta \tag{3.28}$$

$$\bar{\mu}_{ij} = \frac{1}{8\pi^2}\int_0^\pi\int_0^{2\pi}\int_0^{2\pi}\mu_{ij}(\theta,\varphi,\psi)\sin\theta\, d\psi d\varphi d\theta \tag{3.29}$$

**3.3 Constitutive Models With Internal Variables.** One notable feature of ferromagnetic materials is the hysteresis due to energy dissipation, leading to history-dependent material properties. Similar to history-dependent thermodynamics, appropriate internal variables can be defined in the thermodynamics of ferromagnets. Maugin and co-workers [91–94] treated the residual quantities in ferromagnetic materials as the irreversible items in classical plasticity. The residual magnetic quantities and strains were modeled as internal variables in the development of a phenomenological constitutive model for ferromagnetic materials. In addition, homogenization techniques of local physical fields are also used to develop constitutive modeling of ferromagnetic behavior with internal variables [95,96]. By using internal state variables that are chosen in consideration of the crystallographic and magnetic microstructure, Kiefer and Lagoudas [97] derived a phenomenological constitutive model of NiMnGa within the thermodynamic frame, which can capture the magnetic shape memory effect caused by the martensitic variant reorientation process under the dual action of magnetic field and mechanical stress. In the following are summarized two kinds of constitutive models for isotropic and anisotropic magnetic materials, respectively, which were developed by analogy to the flow theory in classical plasticity.

*3.3.1 Constitutive Model Based on the $J_2$ Flow Theory*. It is now well known that there exist similarities in the behavior of ferromagnetic and ferroelectric materials, the latter of which already received a great deal of studies on the electromechanical properties in the past two decades. For example, Bassiouny et al. [98–101] developed a phenomenological ferroelectric constitutive model by adopting the concept of yield surface in the classical theory of plasticity; Kamlah et al. [102–105] simulated the nonlinear behavior by introducing several functions associated with electric domain switching; based on the theory of Bassiouny et al. [98–101] and focusing on the phenomenon of ferroelectric hysteresis, Cocks and McMeeking [106] introduced the concepts of electromechanical yield surface and hardening modulus to establish a new phenomenological constitutive model for ferroelectric hysteresis. Similar to plastic strain in plasticity, there also exist residual quantities (e.g., residual magnetization and strain) in ferromagnetic materials when the external magnetic and mechanical loads are released. By analogy to ferroelectric constitutive models of Cocks and McMeeking [106], the authors of this paper [107–109] proposed a new ferromagnetic constitutive model by introducing residual magnetization and residual strain as internal variables: the evolution law is determined by the Helmholtz free energy function. The strain and magnetization can respectively be divided into two parts: one part reversible and the other irreversible. It is assumed that no coupling between these two parts exists, and the irreversible quantities, such as residual magnetization and strain, do not cause volume change. Upon introducing the yield surface in the space of magnetic field and mechanical stress, $(H_i, \sigma_{ij})$, the constitutive equations can be expressed in the rate form as

$$\dot{\varepsilon}_{ij} = \left( C_{ijkl} + \frac{\partial F}{\partial \sigma_{ij}} A_{kl} \right) \dot{\sigma}_{kl} + \left( q_{kij} + R_k \frac{\partial F}{\partial \sigma_{ij}} \right) \dot{H}_k \tag{3.30}$$

$$\dot{B}_i = \left( q_{ikl} + \frac{\partial F}{\partial H_i} A_{kl} \right) \dot{\sigma}_{kl} + \left( \mu_{ij} + \frac{\partial F}{\partial H_i} R_j \right) \dot{H}_j \tag{3.31}$$

$$A_{ij} = \frac{\partial H^e / \partial \sigma_{ij}}{\dfrac{\partial H^e}{\partial H_k}\left[ \dfrac{\partial H_k^B}{\partial (\mu_0 M_l^r)} \dfrac{\partial H^e}{\partial H_l} + \dfrac{\partial H_k^B}{\partial \varepsilon_{mn}^r} \dfrac{\partial H^e}{\partial \sigma_{mn}} \right] + \dfrac{\partial H^e}{\partial \sigma_{kl}}\left[ \dfrac{\partial \sigma_{kl}^B}{\partial (\mu_0 M_m^r)} \dfrac{\partial H^e}{\partial H_m} + \dfrac{\partial \sigma_{kl}^B}{\partial \varepsilon_{mn}^r} \dfrac{\partial H^e}{\partial \sigma_{mn}} \right]} \tag{3.32}$$

$$R_i = \frac{\partial H^e / \partial H_i}{\dfrac{\partial H^e}{\partial H_k}\left[ \dfrac{\partial H_k^B}{\partial (\mu_0 M_l^r)} \dfrac{\partial H^e}{\partial H_l} + \dfrac{\partial H_k^B}{\partial \varepsilon_{mn}^r} \dfrac{\partial H^e}{\partial \sigma_{mn}} \right] + \dfrac{\partial H^e}{\partial \sigma_{kl}}\left[ \dfrac{\partial \sigma_{kl}^B}{\partial (\mu_0 M_m^r)} \dfrac{\partial H^e}{\partial H_m} + \dfrac{\partial \sigma_{kl}^B}{\partial \varepsilon_{mn}^r} \dfrac{\partial H^e}{\partial \sigma_{mn}} \right]} \tag{3.33}$$

where $\sigma_{ij}^B$ and $H_i^B$ are the back stress and back magnetic field, $e$ and $r$ stand for the reversible and irreversible parts, respectively, $\varepsilon_{ij}^r$ is the residual strain, $M_i^r$ is the residual magnetization, $\varepsilon_{ij} = \varepsilon_{ij}^e + \varepsilon_{ij}^r$, $M_i = M_i^e + M_i^r$, and $F = F(H_k, \sigma_{ij})$ is the yield surface.

The above model can further be simplified by establishing a relation between residual magnetization and residual strain. Suppose that the residual strain is the direct result of residual magnetization, and magnetostriction can be taken as a quadratic function of residual magnetization, there is

$$\varepsilon_{ij}^r = \frac{\varepsilon_0}{2M_0^2}(3M_i^r M_j^r - \delta_{ij} M_k^r M_k^r) \tag{3.34}$$

where $\varepsilon_0$ and $M_0$ are the saturation magnetostriction and magnetization, respectively. A comparison between the theoretical prediction from this model and experimental results is shown in Fig. 28; a close agreement is observed.

*3.3.2 Phenomenological Constitutive Model With Anisotropic Flow Theory*. The isotropic constitutive models described in the preceding section can be extended for the anisotropic cases, including both elastic and magnetic anisotropy. Within the framework of classical elastoplasticity, Taylor [110] developed a plasticity model with a proper physical meaning for polycrystalline solids, but the ensuing computation is time consuming. With phenomenological constitutive models, the computational efforts can

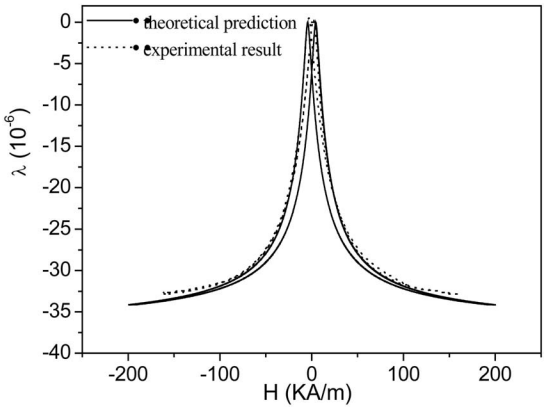


**Fig. 28 Magnetostriction loop of $Ni_6$ without prestress [51]**

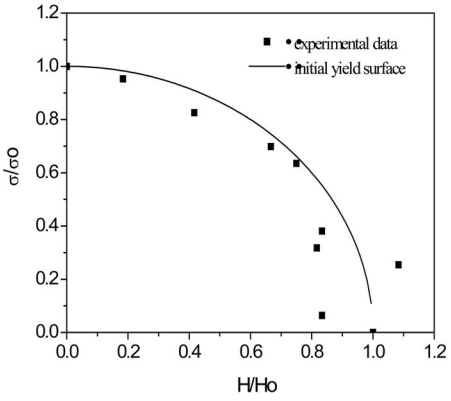


**Fig. 29 Initial yield surface of polycrystalline Terfenol-D [51]**

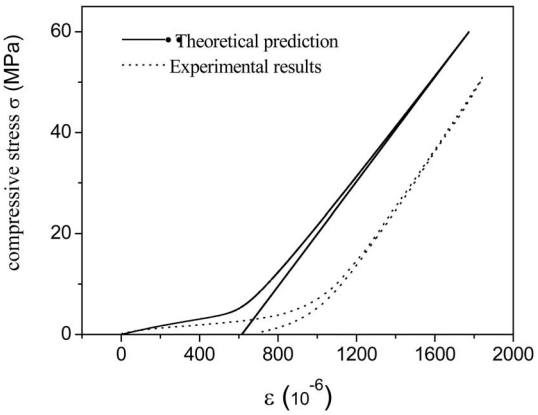


**Fig. 30 Stress versus strain curve for Terfenol-D [51]**

be greatly reduced by introducing a yield surface which, when coupled with flow rules, dictates the plastic behavior of materials. The yield surface, which is usually convex, varies from one model to another. For example, Hosford [111] proposed yield surfaces for isotropic materials, while Hill [112], Budianski [113], Barlat [114], and Barlat and Lian [115] developed anisotropic yield surfaces. In addition to the quadratic form of yield surface, Hershey [116] and Hosford [111] proposed the nonquadratic form for fcc and bcc polycrystalline materials. Karafilles and Boyce [117] developed a general yield criterion, which can be simplified to the other mentioned yield models.

Similar to the Karafilles–Boyce model [117], the authors of this paper developed a general phenomenological constitutive model of ferromagnetism by adopting a nonquadratic yield function [51]. The initial yield surface in the $H-\sigma$ space can be obtained by measuring the magnetization curve under various prestresses and finding the corresponding yield points, as demonstrated in Fig. 29 for oriented polycrystalline Terfenol-D. With residual strain and residual magnetization taken as internal variables, the constitutive equations can then be obtained as

$$\dot{\varepsilon}_{ij} = C_{ijkl}\dot{\sigma}_{kl} + q_{kij}\dot{H}_k + \dot{\varepsilon}^r_{ij} \tag{3.35}$$

$$\dot{B}_i = q_{ikl}\dot{\sigma}_{kl} + \mu_{ij}\dot{H}_j + \dot{J}^r_i \tag{3.36}$$

where a dot represents differentiation with respect to time.

For an anisotropic material, the stress state can be transformed into that of the corresponding isotropic case by means of the isotropic plasticity equivalent (IPE) method. To this end, let the IPE transformation tensor of stress $L^S_{ijkl}$ and magnetic field $L^H_{ij}$ be defined as

$$\tilde{S}_{ij} = L^S_{ijkl}\sigma_{kl}, \quad \tilde{H}_i = L^H_{ij}H_j \tag{3.37}$$

where $\tilde{S}_{ij}$ and $\tilde{H}_i$ are the IPE tensor of stress and magnetic field, while $\sigma_{ij}$ and $H_i$ are the actual stress and magnetic field in the material. The transformation tensors, $L^S_{ijkl}$ and $L^H_{ij}$, assume the following properties:

$$L^S_{ijkl} = L^S_{jikl} = L^S_{jilk}, \quad L^S_{ijkl} = L^S_{klij}, \quad L^S_{ijkk} = 0 \tag{3.38}$$

$$L^H_{ij} = L^H_{ji}, \quad L^H_{ij} = 0 \quad \text{while } i \neq j \tag{3.39}$$

The anisotropic yield function can be obtained by replacing the stress deviator $\tilde{S}_{ij}$ and magnetic field $\tilde{H}_i$ in the isotropic yield function with $\tilde{S}_{ij}$ and $\tilde{H}_i$, respectively, as follows:

$$f(\tilde{S}^0_i, \tilde{H}^0_i) = (1-c)\phi_1(\tilde{S}^0_i, \tilde{H}^0_i) + c\phi_2(\tilde{S}^0_i, \tilde{H}^0_i) - 2Y^{2k} \tag{3.40}$$

The IPE tensor of stress and magnetic field for the cases of mobile hardening and mixing hardening can be obtained in terms of the IPE method as

$$\tilde{S}_{ij} = L^S_{ijkl}(\sigma_{kl} - \sigma^B_{kl}), \quad \tilde{H}_i = L^H_{ij}(H_j - H^B_j) \tag{3.41}$$

The constitutive equations are completed with the experimentally measured yield surface and material parameters. As an example, we [51] have used the experimentally measured magnetomechanical yield surface of Terfenol-D to obtain the constitutive relations. Demonstrated in Fig. 30 is a comparison between theoretical prediction and experimental measurement of the one-dimensional stress versus strain.

## 4 Fracture Mechanics of Soft Ferromagnetic Materials

The fracture behavior of soft ferromagnetic materials and structures under a strong external magnetic field has raised much concern. Cherepanov [118] used the general balance law and invariant integrations to study electromagnetomechanical problems of magnetoelastic media containing cracks. Shindo [119] obtained the crack-tip stress distributions in soft ferromagnetic elastic solids interacting with the magnetic field. Built upon the linearized magnetoelastic theory of Pao and Yeh [24], Shindo studied the problem of an infinitely soft ferromagnetic body containing a center crack in plane strain, with uniform magnetic and mechanical loads applied at infinity normal to the crack surface. Similar to a crack in linear elastic solids, the stress fields around the crack tip assume an inverse square root singularity. Using a similar approach, Shindo [120] obtained the solution to a penny-shaped center crack in an infinite soft ferromagnetic material under an axial magnetic field. According to the analysis, the critical magnetic induction, at which the crack face becomes unstable, is exactly the same as that predicted for the plane strain case. The critical magnetic field $B_{cr}$, in terms of the analysis of Shindo [119], can be estimated by

$$B^2_{cr}/\mu_0 G = \frac{2\mu_r^2}{\chi^2[4\nu - 1 + 2(1-\nu)\chi]} \tag{4.1}$$

where $\mu_0$ and $\mu_r$ are the vacuum permeability and material specific magnetic permeability, $\chi$ is the magnetic susceptibility, and $G$ and $\nu$ are the shear modulus and Poisson's ratio.

The problem of two collinear cracks in an infinite soft ferromagnetic elastic solid [121] was also studied for the case of plane strain. It was found that the critical magnetic induction is consistent with that for a single crack. Furthermore, it was pointed out that the SIF around the inner crack tips is bigger than that around

the outer crack tips, which implies that two collinear Griffith cracks are unstable and may eventually develop into a single crack. Shindo [122] also considered flexural wave scattering at a thickness-through crack in a conducting plate, with a uniform magnetic field applied normal to the crack surface. The magnetic field is found to produce higher singular moments near the crack tip.

The linear magnetoelastic theory was adopted in analyzing a ferromagnetic plate of finite length with a thickness-through crack under bending moments and the transverse uniform magnetic field. The effect of magnetic field on the moment intensity factor was discussed. Results showed that the magnetic field effect becomes more pronounced by increasing either the external magnetic field or the magnetic susceptibility of material [123]. This problem was further experimentally investigated [75]. Theoretical predictions are in good agreement with experimental results.

To find the magnetic effect on fracture parameters, Shindo et al. [74] studied theoretically the stress distribution around a crack in the soft ferromagnetic strip with a uniform magnetostatic field normal to the crack surface by using the linear theory for the soft ferromagnetic elastic materials of multidomain structure. Both the plane stress and plane strain models were formulated by considering the infinitely long strip containing a central crack normal to the edges of the strip. The Fourier transforms were used to reduce the problem to two simultaneous dual integral equations, which can be solved in terms of a single Fredholm integral equation of the second kind. A numerical solution was carried out for obtaining the fracture mechanics parameters such as SIF and energy density. The analysis was also verified by their experiments [74].

Besides Shindo's group, the works on the linear fracture mechanics of soft ferromagnetic elastic solids from some other researchers are summarized as follows. Ang [124] considered a magnetoelastic planar crack in an anisotropic semi-infinite soft ferromagnetic material. The linear magnetoelastic theory of Pao and Yeh [24] was used, but with the magnetostriction effect neglected. It has been established that the result can be reduced to the isotropic case of Shindo [119]. Xu and Hasebe [125] focused on the electromagnetic force in a semi-infinite ferromagnetic induced by electric current: The Maxwell stress tensor was derived from the Lorenz force, and the stress singularity around the crack tip was obtained. Hang and Wang [126] extended the semi-infinite model to the half space case and obtained the complete solution of magnetoelastic field in the soft ferromagnetic solid. Bagdasarian and Hasanian [127] examined the influence of boundary conditions on magnetoelastic interaction in the soft ferromagnetic elastic half-plane that contains a crack subjected to a uniform magnetic field. The discussed boundary of the half-plane include the fastening condition, stress free condition, and mixed conditions. By using the complex variable theory and the linearized formulation of the soft ferromagnetic material of Pao and Yeh [24], Liang et al. [128] and Liang and Shen [129] solved the magnetoelastic field for collinear cracks in a soft ferromagnetic plane with uniform magnetic field and mechanical loads at infinity. Furthermore, Liang et al. [130] studied the magnetoelastic field around an interface crack between two different soft ferromagnetic materials.

In addition to the solutions for a general magnetoelastic field, the energy equilibrium and the energy release rate have been used in ferromagnetic fracture. On the basis of the magnetoelastic coupling theory developed by Maugin [5] and Eringen and Maugin [6], Sabir and Maugin [131] and Fomethe and Maugin [132] established the path-independent integrals for both soft and hard ferromagnets. Wang and Shen [133] extended the notion of energy momentum to soft ferromagnets and obtained the balance law of energy and path-independent integrals: This theory was subsequently used in analyzing crack problem in ferromagnetic materials.

There exist obvious limitations in the linear fracture mechanics mentioned above. For example, slit crack tip may be subject to some kind of passivation after deformation. Magnetic materials

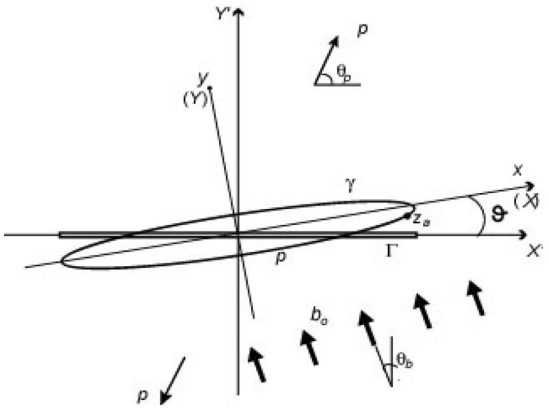


**Fig. 31 An infinite plane with a center-through crack [131]**

usually saturate under an intense magnetic field, which is actually the case around the crack tip. Also, the plastic behavior should be involved when considering crack growth in metallic ferromagnetics. Recent progress on the nonlinear magnetoelastic fracture have been achieved and are therefore particularly summarized in the following subsections. Firstly, upon magnetoelastic deformation, the crack distortion and tip passivation were considered in theoretical models so as to eliminate the singularity of SIF obtained from the linear analysis [134–136]. Secondly, when analyzing the cracklike flaws in magnetic materials of giant magnetostriction, the nonlinearity of magnetostriction has been taken into account [137]. Furthermore, the saturation of magnetization and magnetostrain has been included on the basis of linear magnetoelastic analysis with cracklike flaw [138]. Finally, with regard to the magnetic-aided crack growth in ferromagnetic soft alloy, the linear magnetoelastic analysis was extended to the nonlinear formulation by including Dugdale's treatment of the plastic zone in metals [76].

**4.1 Nonlinearity due to Crack Configuration Variation.** The disagreement between theoretical prediction and experimental measurement is partially attributable to the mathematical idealization of a sharp line crack. Liang et al. [134] did not adopt the assumption of Pao and Yeh [24] that the magnetic field coupled with the deformation is far smaller than the magnetic field in the rigid state. In their treatment, the magnetic field variation around the crack tip was considered to be of the same order of magnitude as that in the rigid state since the deformation gradient is large in the vicinity of the crack tip. The equilibrium equation then becomes as follows:

$$\sigma_{ij,i} + 2\mu_0 M_k H_{j,k} + \mu_0 M_j H_{k,k} = 0 \tag{4.2}$$

where $M_k$ and $H_k$ are the magnetization and magnetic field, respectively, and the stress tensor $\sigma_{ij}$ satisfies

$$\sigma_{ij} = \lambda u_{k,k}\delta_{ij} + G(u_{i,j} + u_{j,i}) \tag{4.3}$$

where $\lambda$ and $G$ are the Lame constants of elastic solid. Meanwhile, the line crack is considered to be an elliptical contour after distortion.

Liang et al. [135] and Liang [136] further introduced a rotation angle into the configuration variation of the original line crack. As shown in Fig. 31, an in-plane magnetic field $b_0$ and a mechanical tension load $p$ are applied at infinity for an infinite plane of soft ferromagnetic material containing a through crack. Here, $\theta_b$ and $\theta_p$ are the inclination angles for the magnetic field and the mechanical load, respectively. The original line crack lies on the $O'X'$ line prior to deformation, which deforms into an ellipse, denoted by $\gamma$ in the $X'O'Y'$ coordinates (Fig. 31). Generally, three parameters suffice to determine the elliptical crack surface, i.e., the semiaxes $\alpha$ and $\beta$ and the inclination angle of the major axis

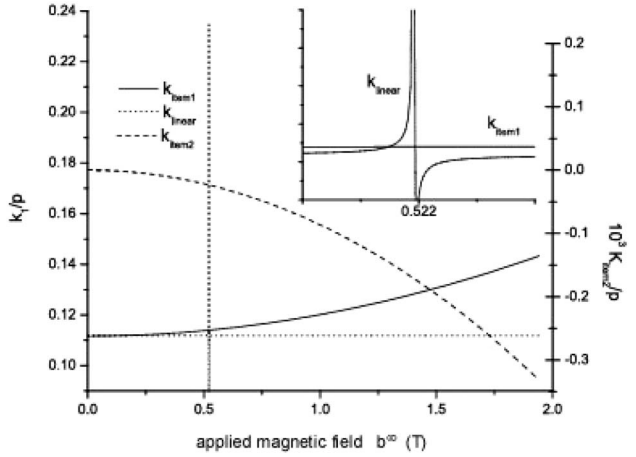


**Fig. 32 The variation of SIF with the magnetic field [131]**

of the ellipse with respect to the original coordinate, $\vartheta$.

The analysis of Liang et al. [135] and Liang [136] reveals that both the magnetic and stress fields concentrate in the vicinity of the crack tip but are not singular. The stresses in the annular area around the crack tip contain two items: one item varying with $1/\sqrt{r}$ and the other with $1/r$, where $r$ is the distance measured from the crack tip. Accordingly, two parameters $k_{\text{item1}}$ and $k_{\text{item2}}$ can be assigned to identify the magnitude for the item with $1/\sqrt{r}$ and that with $1/r$, respectively. Plotted in Fig. 32 is an example for the variation of the SIF with the magnetic field, where the shear modulus $G=78$ GPa, the magnetic susceptibility $\chi=500$, the Poisson ratio $\nu=0.3$. The stresses and magnetic field at infinity are $\sigma_{yy}^{\infty}=1$ MPa, $\sigma_{xx}^{\infty}=\sigma_{xy}^{\infty}=0$, and $b_x^{\infty}=0$. $k_{\text{linear}}$ is the SIF obtained from the common linear magnetoelasticity. It is seen from Fig. 32 that $k_{\text{item1}}$ varies smoothly, and no singularity exists as the magnetic field increases, which is different from that estimated by the linear magnetoelasticity model.

**4.2 Magnetoelastic Analysis With Nonlinear Magnetostrictive Effect [137].** Some soft ferromagnetics such as the giant magnetostrictive alloy of RE and iron exhibit significant nonlinear magnetostriction effect when subjected to an external magnetic field. To account for the nonlinear effect in the analysis of magnetoelastic fracture, we [137] developed a model on the basis of the magnetic force model of Brown [2] and the magnetoelastic analysis for soft ferromagnetics of multidomain developed by Pao and Yeh [24]. In this analysis, linear magnetization and the standard square constitutive model of magnetostriction were adopted. It is found that the stress field concentrates in an annular area surrounding the elliptical crack tip and the mode I SIF can be defined as

$$K_{\text{I}}=\left[\frac{\delta_{\text{I}}}{2}(1+\Delta_1^2)+\frac{\kappa}{2}(1+\Delta_1)^2-\delta_{\text{II}}\Delta_2^2\right]B^{\infty}\overline{B^{\infty}}\sqrt{\pi a} \tag{4.4}$$

where

$$\kappa=S-\frac{\delta_{\text{I}}}{4\left[\dfrac{\nu(1-\nu)}{1-2\nu}+\dfrac{1-\nu}{2}\right]},\quad S=\frac{1-(1+2\nu)q}{4}E'm_{11},$$
$$E'=\frac{E}{1-\nu^2},\quad q=-\frac{m_{21}}{m_{11}} \tag{4.5}$$

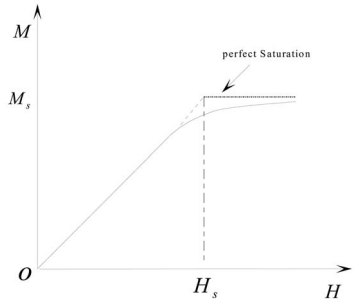


**Fig. 33 The magnetization curve of the perfect saturation model [133]**

$$\Delta_1=\frac{\tau-1}{\tau+1},\quad \Delta_2=\frac{1}{\tau+1},\quad \tau=\frac{b\mu_1}{a\mu_2},\quad \delta_{\alpha}=\frac{\chi_{\alpha}}{\mu_0(1+\chi_{\alpha})^2},\quad \alpha=\text{I,II} \tag{4.6}$$

Here, $a$ and $b$ are the major and minor semiaxes of the elliptical crack; $B^{\infty}=\mu_1 H^{\infty}$ is the magnetic induction at infinity; $\mu_1$ and $\mu_2$ are, respectively, the magnetic permeability of matrix outside the ellipse and the medium inside the elliptical crack while $\chi_{\text{I}}$ and $\chi_{\text{II}}$ are, respectively, their magnetic susceptibility; $\delta_{\text{I}}$ and $\delta_{\text{II}}$ are combined parameters; $\mu_0$ is the permeability of vacuum; $E$ and $\nu$ are the Young modulus and Poisson ratio of the material outside the elliptical crack, while $m_{11}$ and $m_{21}$ are the magnetostrictive constants, which physically represent the magnetostrain induced by a unit magnetic induction in the parallel and perpendicular directions of the external magnetic field. The subscripts I and II refer to the media outside and inside the crack, respectively.

As indicated in Eq. (4.4), the SIF is determined by both the magnetostrictive behavior and the magnetic force effect, where magnetostrictive coefficients are included in the parameter $\kappa$. Generally speaking, except for slit cracks, the magnetostrictive effect cannot be neglected, especially for those materials of great magnetostriction. A slit crack is the limit case of an elliptical crack. When the minor semiaxis of an elliptical crack becomes zero ($b=0$, it reduces to a slit crack, with $\Delta_1=-1$ and $\Delta_2=1$. It can then be shown that the magnetic field is homogeneous for the entire plane and equals the externally applied magnetic field at infinity. The stress field has a singularity, the same as that of the classical Griffith crack. For soft ferromagnetic materials with a negligibly small magnetostrictive effect, the SIF in Eq. (4.4) can be simplified as

$$K_{\text{I}}=\delta_{\text{I}}B^{\infty}\overline{B^{\infty}}\sqrt{\pi a} \tag{4.7}$$

This expression is independent of magnetostrictive coefficients, implying that the magnetostrictive effect can be neglected in the fracture analysis of soft ferromagnetics with small magnetostrictive effect. This seems to be consistent with the conclusions reached by Shindo [119].

**4.3 Magnetoelastic Analysis With Magnetostrain Saturation [138].** Magnetostrain can generally be regarded as a quadratic function of the magnetic field if it is not very strong. When the magnetic field becomes intense, magnetostrain approaches the saturation point, $\varepsilon_s$, which is a material constant. Figure 33 shows the magnetization of a typical soft ferromagnetic, where magnetization is considered to be linear with the magnetic field until the saturation point is reached; $M_s$ is the corresponding saturated magnetization and $H_s$ refers to the magnetic field at which the magnetization saturates, both of which are material constants. The magnetic field near the crack tip may be larger than $H_s$ due to the concentration effect even when the applied magnetic field is smaller than $H_s$. The majority portion of the plane can be treated as linearly magnetized except for a small volume around the crack

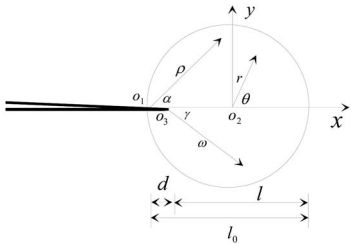


**Fig. 34 The size and position of the magnetization saturation zone [133]**

tip. This is the so-called small-scale magnetic-yielding condition.

As schematically illustrated in Fig. 34, the saturation zone around the crack tip may be approximated as a circular cylinder of radius $r_s$, where

$$d = b\sqrt{\frac{2r_s}{a}}, \quad = 2r_s - b\sqrt{\frac{2r_s}{a}} \tag{4.8}$$

$$r_s = \frac{1}{2\pi}\left(\frac{K_H}{H_s}\right)^2, \quad H = \frac{1}{2}\frac{a(1+\Delta_1)}{\sqrt{2ar+b^2}}H^{\infty} \tag{4.9}$$

It can then be shown that the hoop stress on the crack extension line inside the saturation zone is given by

$$\sigma_{22} = \frac{A_1 + D_3}{d+\omega} + 3\frac{D_3}{r_s}\frac{d}{d+\omega} - \frac{d\cdot D_3}{(d+\omega)^2} + 2\frac{D_3}{r_s}\ln\frac{d+\omega}{r_s} \tag{4.10}$$

where

$$D_3 = -\frac{Gr_s}{4(1-\nu)}(\varepsilon_\alpha - \varepsilon_\rho) \tag{4.11}$$

$$A_1 = \frac{(3-2\nu)p_5}{4(1-\nu)} + \frac{(-3+2\nu)Gr_s}{4(1-\nu)}(\varepsilon_\alpha - \varepsilon_\rho) \tag{4.12}$$

$$p_5 = -\frac{G}{8}(m_{11}-m_{21})(1+\Delta_1)^2 a(\mu_1 H^{\infty})^2 \tag{4.13}$$

$$\varepsilon_\rho = (1+\nu)m_{21}M_s^2, \quad \varepsilon_\alpha = (m_{11}+\nu m_{21})M_s^2 \tag{4.14}$$

The above theoretical model was used to interpret the experimental results of soft ferromagnetic materials [49,73].

**4.4 Dugdale Crack Model for the Soft Ferromagnetic Materials [76].** Shindo et al. [76] had studied the problem of magnetic-aided crack growth in soft ferromagnetic alloys, where the Dugdale small-scale mechanical yielding condition was adopted in treating the plastic deformation around the crack tip. An infinite soft ferromagnetic plane with a finite crack was considered. A uniform tensile stress and a uniform magnetic field of magnetic induction $B_0$ normal to the crack surface are applied at infinity. The tensile stress (the sum of the magnetoelastic and Maxwell ones) on the plastic yielding planes ahead of the crack tip is assumed to be uniform and prescribed. By using a dipole model for the magnetization, this problem can be formulated in the perturbation state with the mixed boundary conditions. By means of Fourier transform, the mixed boundary problem can be reduced to two simultaneous integral equations, from which the final solution including displacements and the SIF can be solved. The crack opening displacement $\mathrm{COD}_1(x)$ within the yield zone can be determined. Based on the accumulated plastic displacement or accumulated plastic work criterion, the crack growth is assumed to start when the accumulated plastic displacement $D_T$ of a certain point equals a critical value $D_c$. Then the CGR in the small-scale yielding condition can finally be obtained as

$$\frac{da}{dN} = \frac{\pi y_0^4}{192FD_c(\sigma_{y0} - \mu b_c^2/2)^3}\Delta k_{h1}^4 \tag{4.15}$$

where

$$F = 2\mu y_0\left(\frac{\kappa+\mu}{\kappa+2\mu}\right) \tag{4.16}$$

$$y_0 = 1 - \frac{1}{2}\left(\frac{\kappa+2\mu}{\kappa+\mu}\right)\mu_r\left(\frac{\chi b_c}{\mu_r}\right)^2 \tag{4.17}$$

$$b_c^2 = \frac{B_0^2}{\mu\mu_0} \tag{4.18}$$

where $da/dN$ is the CGR per cycle and $N$ is the number of loading cycles. $\kappa=\lambda$ for plane strain and $\kappa=2\lambda\mu/(\lambda+2\mu)$ for plane stress. $\lambda$ and $\mu$ are the Lame constants. $\mu_r=1+\chi$ is the specific magnetic permeability, and $\chi$ is the magnetic susceptibility. $a$ is half of the crack length, and the plastic yielding zone lies on the segment of $a<|x|<c$, where the crack is on the $x$ axis.

## 5 Effective Magnetostriction of Ferromagnetic Composites: Micromechanics Approach

**5.1 Equivalent Modulus of Ferromagnetic Composites.** Although soft ferromagnetic materials have been widely used, some materials (e.g., giant magnetostrictive alloy of RE and iron) are very brittle and not suitable for dynamic use due to large eddy-current loss. Consequently, in recent years, ferromagnetic composites with soft matrix and ferromagnetic particulate inclusions have received much attention. Of all the effective properties, the effective magnetostriction is a parameter of considerable significance. Both theoretical efforts and experiments have been conducted to study the effective magnetostriction. Amongst different theoretical models, those based on the micromechanics approach have an explicit physical background. In the following, the equivalent moduli of ferromagnetic composites obtained from the micromechanics approach are summarized.

Nan [139] developed a theoretical work for the analysis of piezoelectric and piezomagnetic composite by means of the Green's function and permutation method; the linear coupled magneto-electroelastic constitutive relation was adopted. With a special averaging scheme, the following effective constitutive relations were obtained:

$$\begin{bmatrix}\langle\boldsymbol{\sigma}\rangle\\ \langle\mathbf{D}\rangle\\ \langle\mathbf{B}\rangle\end{bmatrix} = \begin{bmatrix}\mathbf{C}^* & -\mathbf{e}^{T*} & -\mathbf{q}^{T*}\\ \mathbf{e}^* & \boldsymbol{\varepsilon}^* & \boldsymbol{\alpha}^*\\ \mathbf{q}^* & \boldsymbol{\alpha}^{T*} & \boldsymbol{\mu}^*\end{bmatrix}\begin{bmatrix}\langle\mathbf{s}\rangle\\ \langle\mathbf{E}\rangle\\ \langle\mathbf{H}\rangle\end{bmatrix} \tag{5.1}$$

where $(\mathbf{C}^*, \mathbf{e}^*, \mathbf{q}^*, \boldsymbol{\varepsilon}^*, \boldsymbol{\alpha}^*, \boldsymbol{\mu}^*)$ are, respectively, the effective elastic moduli, piezoelectric coefficient, piezomagnetic coefficient, dielectric permittivity, magnetoelectric coefficient, and magnetic permeability; $\langle\ \rangle$ represents the volume average; $\boldsymbol{\sigma}$ is the stress tensor, $\mathbf{s}$ the strain tensor, $\mathbf{D}$ the electric displacement, $\mathbf{e}$ the electric field, $\mathbf{B}$ the magnetic flux density, and $\mathbf{H}$ the magnetic field. However, it appears that this work does not consider the interaction amongst inhomogeneities

Huang and co-workers [140–143] developed a unified method for an analysis of piezoelectric/piezomagnetic composites, adopting the following linear piezoelectric/piezomagnetic constitutive laws:

$$\sigma_{ij} = C_{ijkl}\varepsilon_{kl} - e_{nij}E_n - q_{nij}H_n$$

$$D_i = e_{imn}\varepsilon_{mn} + \kappa_{in}E_n + \lambda_{ni}H_n$$

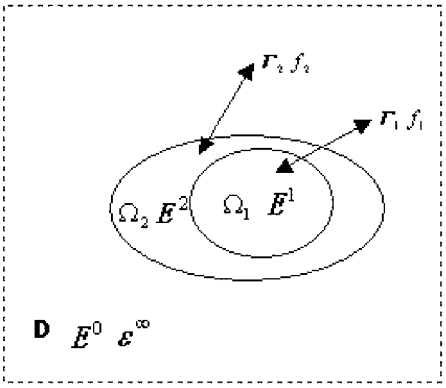


**Fig. 35 Schematic of a double-inclusion model [142]**

$$B_i = q_{imn}\varepsilon_{mn} + \lambda_{in}E_n + \Gamma_{in}H_n \tag{5.2}$$

where $C_{ijkl}$, $e_{nij}$, $q_{nij}$, $\kappa_{in}$, $\Gamma_{in}$, and $\lambda_{ni}$ are the elastic parameters, piezoelectric parameters, piezomagnetic parameters, dielectric constants, and permeability and magnetoelectric constants, respectively. By supposing that the composite reinforcements are ellipsoidal in shape, a unified form of the magnetoelectroelastic Eshelby tensor as well as the magnetic, electric, and elastic fields and the concentrating tensor around the inclusion were obtained. The overall properties of the composite were examined by analogy to the Mori–Tanaka average-field theory.

Extending the double-inclusion model for elasticity to treat the multicoupling fields of magnetoelectroelasticity, Li and Dunn [144] and Li [145] studied the magnetoelectroelastic behavior of piezoelectric and piezomagnetic composites. The effective modulus by means of the generalized double-inclusion model is as follows:

$$E^*_{iJAb} = E_{iJMn}[I_{MnKl} + (S^2_{MnCd} - I_{MnCd})A_{CdKl}] \cdot [I_{KlAb} + S^2_{KlEf}A_{EfAb}]^{-1} \tag{5.3}$$

Here, $E^*_{iJAb}$ is the effective magnetoelectroelastic tensor, $E_{iJMn}$ is the magnetoelectroelastic tensor of the matrix $S^2_{KlEf}$ is the Eshelby tensor of double inclusion, $I_{MnKl}$ is the identity tensor, and $A_{AbMn}Z^\infty_{Mn} = \Sigma^2_{r=1} f_r Z^T_{Ab}|_r$, where $Z^T_{Ab}$ is the equivalent eigenfield, which can be derived through the consistency condition, and $f_r$ is the volume fraction of the $r$ phase.

We [146–148] have theoretically investigated the effective properties of ferromagnetic composites with giant magnetostrictive particles and the nonmagnetostrictive matrix, where the saturated magnetostriction of the magnetostrictive phase was treated as an eigenstrain. By means of the double-inclusion model, the effective modulus of the composite was obtained. As demonstrated in Fig. 35 an ellipsoidal inclusion $\Omega_1$ was embedded into another ellipsoidal inclusion $\Omega_2$ to form the double inclusion. Let the volume fractions of phase $\Omega_1$ and phase $\Omega_2$ be denoted by $f_1$ and $f_2$, respectively. The double inclusion was then inserted into an infinite medium $D$, with a homogeneous strain field $\varepsilon^\infty_{ij}$ applied at infinity. The equivalent elastic modulus of the composite was then obtained as

$$E^*_{ijkl} = E^0_{ijrs}[I_{rspq} + (S^2_{rsmn} - I_{rsmn})(f_2A^2_{mnpq} + f_1A^1_{mnpq})] \times [I_{pqkl} + S^2_{pqcd}(f_2A^2_{cdkl} + f_1A^1_{cdkl})]^{-1} \tag{5.4}$$

where $E^*_{ijkl}$ is the effective modulus of the composite, $E^1_{ijkl}$, $E^2_{ijkl}$, and $E^0_{ijkl}$ are the elastic modulus of inclusion $\Omega_1$, inclusion $\Omega_2 - \Omega_1$, and the infinite medium $D$, respectively; $S^1_{ijkl}$ and $S^2_{ijkl}$ are the Eshelby tensor of inclusion $\Omega_1$ and inclusion $\Omega_2$, respectively; $I_{rspq}$ is the identity tensor of order 4.

**5.2 Effective Magnetostriction of Magnetostrictive Composites.** Composites with giant magnetostrictive particles of RE elements are well known for large magnetostriction, good mechanical properties, and small eddy-current loss. Pinkerton et al. [149] fabricated the magnetostrictive composite of $SmFe_2/Fe$ and $SmFe_2/Al$, and the effect of individual constituents on the effective magnetostriction of the composite was studied. They found that the machining property of the composite was improved significantly in comparison with the single magnetostrictive phase $SmFe_2$. Chen et al. [150] suggested that the matrix should be so chosen to have a modulus close to that of the magnetostrictive phase. Duenas and Carman [151] designed and fabricated a magnetostrictive composite made of resin and Terfenol-D particles. They found that there exists an optimum volume fraction of the Terfenol-D phase for maximum effective magnetostriction. By choosing Terfenol-D as the magnetostrictive phase and either resin or glass as the matrix, Guo et al. [152] developed two different kinds of magnetostrictive composites. They tested the static and dynamic magnetomechanical behavior of the composite and found that its magnetomechanical coupling coefficient $k_{33}$ depends on the elastic modulus of resin: It is possible to find an optimal $k_{33}$ by selecting a proper resin. Ryu et al. [153] fabricated the magnetoelectric laminate composites by stacking and bonding a piezoelectric transducer (PZT) disk and two magnetostrictive Terfenol-D disks. This kind of composite can be operated with a high magnetoelectric effect.

On the modeling front, Nan et al. [154–156] proposed an analytical model for the effective magnetostriction of magnetostrictive composites by means of the Green function method. The effective magnetostriction can be calculated by

$$\bar{\varepsilon} = (C^*)^{-1}\{\bar{\sigma} - \langle[(C^* - C)(I - G^uC')^{-1}G^u - I]C\lambda\rangle\} \tag{5.5}$$

where $C$ is the stiffness of the inhomogeneous medium and can be expressed by $C(x) = C^0 + C'$ in which $C^0$ is the stiffness of a reference homogeneous medium, $C'$ is the stiffness disturbance due to inhomogeneity, $G^u$ is the modified Green function for the displacement, $C^*$ is the effective stiffness of the composite, and $\lambda$ is the saturated magnetostriction. Armstrong [157,158] developed a method to estimate the effective magnetostriction of magnetostrictive particle reinforced composite by means of the magnetic free energy, on the assumption that the matrix is nonmagnetic and the composite is subjected to a homogeneous magnetic field at infinity. The magnetic free energy is supposed to be composed of three parts: the magnetic energy, the magnetocrystalline energy, and the magnetoelastic energy. The macroscale deformation of the composite is determined by the Mori–Tanaka averaging scheme. In addition, for the case that the matrix is nonmagnetostrictive, Herbst et al. [159] developed a relatively simple model for the effective magnetostriction.

The double-inclusion method [160,161] was generalized to investigate the effective magnetostriction of magnetostrictive composites, where the saturated magnetostriction of the material was treated as an eigenstrain [146–148]. The equivalent magnetostriction can be obtained through the average strain field of the composite with an eigenstrain. The effective magnetostriction is estimated as follows:

$$\bar{\varepsilon}^{\mathrm{ms}} = \langle \boldsymbol{\varepsilon}^H \rangle = f\{\mathbf{S}:[\mathbf{A}^{\mathrm{I}}:(\mathbf{S} - \mathbf{I}) + \mathbf{I}] - (\mathbf{I} + f\mathbf{S}:\mathbf{A}^{\mathrm{I}}):[(\mathbf{S} - \mathbf{I}):\mathbf{A}^{\mathrm{I}} + \mathbf{I}]^{-1}:(\mathbf{S} - \mathbf{I}):[\mathbf{A}^{\mathrm{I}}:(\mathbf{S} - \mathbf{I}) + \mathbf{I}]\}:\boldsymbol{\varepsilon}^{\mathrm{ms}} \tag{5.6}$$

where $\mathbf{A}^1$ is the strain concentration tensor of the inclusion $\Omega_1$ (see Fig. 5), $\mathbf{S}$ is the Eshelby tensor, $\mathbf{I}$ is the identity tensor, and $f$ is the volume fraction of the inclusion $\Omega_1$. If the particles are made of a cubic phase crystal, the magnetostrain field $\boldsymbol{\varepsilon}^{\mathrm{ms}}$ in the local coordinates of the crystalline axes becomes

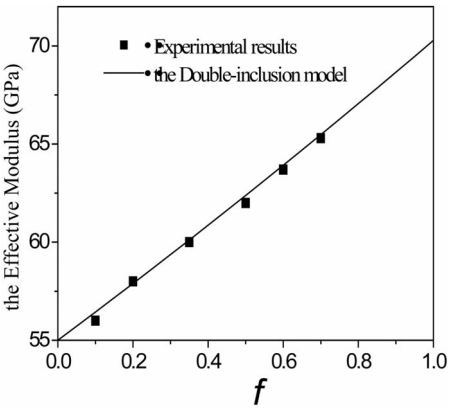


**Fig. 36 Effective modulus plotted against volume fraction [142]**

$$\varepsilon_{ij}^{\mathrm{ms}} = \begin{cases} \lambda^{\alpha} + \dfrac{2}{3}\lambda_{100}\left(\alpha_{3i}^2 - \dfrac{1}{3}\right), & i = j \\ \dfrac{3}{2}\alpha_{3i}\alpha_{3j}\lambda_{111}, & i \neq j \end{cases} \tag{5.7}$$

where $\lambda_{100}$, $\lambda_{111}$, and $\lambda^{\alpha}$ are the magnetostrictive coefficients of the cubic phase crystal, and $(\alpha_{ij})$ is the transformation tensor from the local coordinate $X_j'$ to the global coordinate $X_i$. The equivalent magnetostriction of the composite is thence obtained as

$$\bar{\lambda}_s = \frac{2}{3}(\bar{\varepsilon}_{\parallel}^{\mathrm{ms}} - \bar{\varepsilon}_{\perp}^{\mathrm{ms}}) \tag{5.8}$$

where $\bar{\varepsilon}_{\parallel}^{\mathrm{ms}}$ and $\bar{\varepsilon}_{\perp}^{\mathrm{ms}}$ are the magnetostrain in the direction parallel and perpendicular to the external magnetic field, respectively. It is seen from the above results that the equivalent magnetostriction is dependent on the magnetostrictive coefficient of the crystal, the inclusion shape, and the elasticity of the matrix. For two specific examples of magnetostrictive composite of $SmFe_2/Al$ and $SmFe_2/Fe$ with Terfenol-D/glass, the theoretical predictions and experimental data are compared in Figs. 36 and 37, respectively.

To establish the quantitative relation between the effective properties of a composite and the properties of its constituents, we [162] systematically studied the effect of magnetic properties, including the permeability of each constituent, on the overall magnetostriction. The results indicate that magnetostrictive composites can be roughly divided into two kinds: one kind in which the the matrix is either nonmagnetic or has very low magnetostriction,

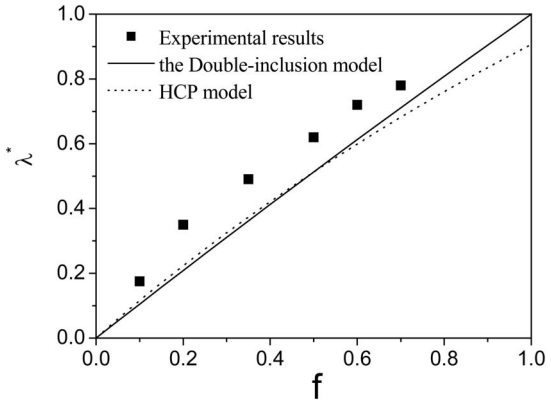


**Fig. 37 Equivalent magnetostriction plotted against volume fraction [142]**

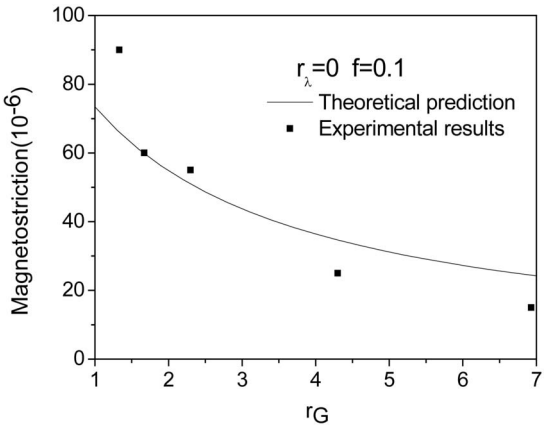


**Fig. 38 Composite magnetostriction plotted against elastic modulus ratio $r_G$ [157]**

whereupon the effective magnetostriction of the composite is independent of the permeability of constituents, and another kind in which the reinforcement has a magnetostriction similar to that of the matrix, whereupon the effective magnetostriction of the composite depends on both the elastic and magnetic parameters of each constituent and also the volume fractions. Unlike the first kind, in a certain range, the effective magnetostriction of the second kind of composites can be improved by increasing the matrix permeability. Comparisons are made between theoretical predictions and experimental data published in the literature, as shown in Figs. 38 and 39 with good agreement.

## 6 Concluding Remarks

Functional ferromagnetic materials have already been widely used in engineering. The newly developed giant magnetostrictive alloy of RE and iron and ferromagnetic shape memory alloys show great potential in the development of a new generation of magnetomechanical devices, owing to their superior properties, such as the giant magnetostriction, large energy density, etc. The magnetoelastic coupling constitutive behavior and the associated fracture problems of these materials under the dual action of magnetic and mechanical loads have received increased attention in recent years. Great progress in both theoretical and experimental aspects has been achieved, as reviewed in this article. However, further research is needed, summarized as follows.

(1) Much progress has been made in the magnetomechanical

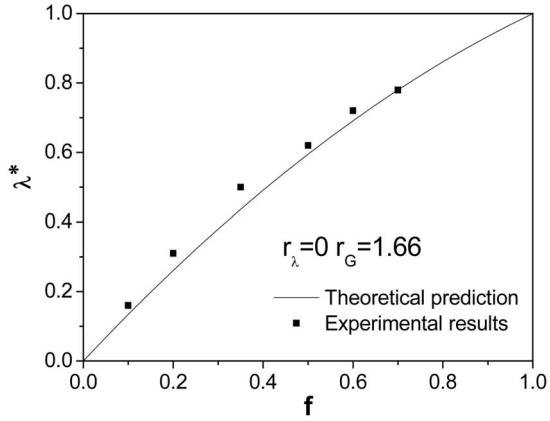


**Fig. 39 Effective magnetostriction $\lambda^*$ plotted against volume fraction $f$ [157]**

experiments of ferromagnetic materials, especially the magnetomechanical setup, from which the dual action of magnetic and mechanical loads can be simultaneously applied. However, experimental techniques still need to be improved. The strain measurement, for example, is usually conducted by means of the strain gauge, regardless of the magnetic field. As one knows, electromagnetic interference will directly change the authenticity of the testing strain data. In order to reduce the external disturbance, some available measures, e.g., the shielded wires, can be adopted. A more advanced and accurate method should be introduced into the experiments with the magnetic field. For example, the noncontact techniques and other testing methods free from interference can be included in the measurement of displacement and magnetostrain; therefore, the electromagnetic disturbance can be completely avoided.

(2) The mechanism of the magnetic-field-induced transformation in NiMnGa should be further studied. As was pointed out by Liang et al. [70], the direct magnetic effects on martensitic transformation were very small, while stress-induced transformations are appreciable. However, open literature is rather limited on this subject. It is therefore believed that much more work is needed. To address the role of magnetic field in transformation in NiMnGa, carefully designed experiments are required for illustrating this problem, where an examination of the magnetic force aroused by nonuniformity of the magnetic field should be particularly involved.

(3) As far as the magnetic effect on fracture parameters is concerned, experiments in the open literature present two kinds of completely different results. Some experiments showed no measurable effect, while others found a significant effect. In analyzing these completely different experimental results, Shindo's group argued that magnetic effect depends on candidate specimen materials, the direction of magnetic field, and loading conditions. Naturally, further understanding must rely on more experiments with different candidate materials. For example, the specimen materials are usually of little magnetostriction. Further experiments should be carried out with the candidate materials of large magnetostriction. Other loading conditions, e.g., inclined magnetic field over the crack surface, are also helpful in clarifying this problem and should be employed in experiments.

(4) The analysis of a dynamic magnetoelastic fracture with crack growth is still insufficient. For example, the Dugdale crack model [76] for the soft ferromagnetic materials with crack growth predicts a nonlinear relation for CGR versus magnetic field, while the experiment shows a linear relation. The developed models, including those for magnetoelastic stresses around a crack tip, are mainly based on the linearized magnetoelastic theory of soft ferromagnetic materials with multidomain, where many important features of the ferromagnetic material, such as ferromagneticity and magnetic hysteresis, were ignored. More efforts should further be put on theoretical models for dynamic magnetoelastic fracture and also in clarifying the magnetic effect on fatigue mechanism with crack growth. In addition, the understanding of deformation and fracture of hard ferromagnets is still very limited.

(5) Most analytic models for ferromagnetic composites are based on a linear assumption with regard to magnetostriction, whether a Green function method or an equivalent eigenstrain method. To consider the interaction between magnetostrictive phase and matrix, linear piezomagnetic equations are usually involved in the theoretical model. However, magnetostrictive materials, especially those of giant magnetostriction, are characterized by the nonlinear behavior under a magnetic field. Deep insight into the overall behavior of ferromagnetic composites should be based on material nonlinear properties and phase interaction. On the other hand, a comparison between theoretical prediction and experimental results are still not satisfactory. A general three-dimensional analysis incorporating the nonlinear constitutive behavior of the magnetostrictive phase is yet to be developed.

## Acknowledgment

Partial financial support from the National Natural Science Foundation of China (Grant Nos. 10025209, 10132010, 10102007, 90208002, 10402028, and 10328203) and from the Research Grants Council of the Hong Kong Special Administrative Region, China (RGC, Project No. HKU 7063/01E) is acknowledged. The authors are also grateful for the support by the Key Project of Chinese Ministry of Education (Grant No. 0306) and the National Basic Research Program of China (Grant No. 2006CB601202).

## References

[1] Carroll, M. M.1986, "The Foundation of Solid Mechanics," Appl. Mech. Rev., **38**(10), pp. 1301–1308, in Chinese.
[2] Brown, W. F., Jr., 1966, *Magnetoelastic Interactions*, Springer-Verlag, New York.
[3] Pao, Y. H., 1978, *Electromagnetic Force in Deformable Continua*, Mechanics Today, N. Nasser, ed. Pergamon, Bath.
[4] Moon, F. C., 1984, *Magneto Solid Mechanics*, Wiley, New York.
[5] Maugin, G. A., 1988, *Continuum Mechanics of Electromagnetic Solids*, North-Holland, Amsterdam.
[6] Eringen, A. C., and Maugin, G. A., 1989, *Electrodynamics of Continua*, Springer-Verlag, New York, Vols. 1 and 2.
[7] Zhou, Y. H., and Zheng, X. J., 1999, *Mechanics of the Electromagnetic Solids Structure*, Science, Beijing, in Chinese.
[8] Watanabe, K., and Motokawa, M., 2001, *Materials Science in Static High Magnetic Fields*, Springer-Verlag, Berlin.
[9] Wohlfarth, E. P., 1980, *Ferromagnetic Materials: A Handbook on the Properties of Magnetically Ordered Substances*, North-Holland, Amsterdam, Vols. 1 and 2.
[10] Jiang, Z., 1992, "Development of the Giant Magnetostrictive Compound of Rare Earth and Iron," Chinese Journal of Rare Earth, **12**, pp. 19–26, in Chinese.
[11] Nan, C. W., Li, M., Feng, X., and Yu, S., 2001, "Possible Giant Magnetoelectric Effect of Ferromagnetic Rare-Earth-Iron-Alloys-Filled Ferroelectric Polymers," Appl. Phys. Lett., **78**, pp. 2527–2529.
[12] Nan, C. W., and Weng, G. J., 1999, "Influence of Microstructural Features on the Effective Magnetostriction of Composite Materials," Phys. Rev. B, **60**, pp. 6723–6730.
[13] Bednarek, S., 1999, "The Giant Magnetostriction in Ferromagnetic Composites Within an Elastomer Matrix," Appl. Phys. A: Mater. Sci. Process., **68**, pp. 63–67.
[14] Kokorin, V. V., and Chernenko, V. A., 1989, "Martensitic Transformation in Ferromagnetic Heusler Alloy," Phys. Met. Metallogr., **68**, pp. 1157–1160.
[15] O'Handley, R. C., 1998, "Model for Strain and Magnetization in Magnetic Shape-Memory Alloys," J. Appl. Phys., **83**, pp. 3263–3270.
[16] Sozinov, A., Likhachev, A. A., Lanska, N., and Ullakko, K., 2002, "Giant Magnetic-Field-Induced Strain in NiMnGa Seven-Layered Martensitic Phase," Appl. Phys. Lett., **80**, pp. 1746–1748.
[17] Wu, G. H., Wang, W. H., Chen, J. L., Ao, L., Liu, Z. H., Zhan, W. S., Liang, T., and Xu, H. B., 2002, "Magnetic Properties and Shape Memory of Fe-Doped $Ni_{52}Mn_{24}Ga_{24}$ Single Crystals," Appl. Phys. Lett., **80**(4), pp. 634–636.
[18] Wang, W. H., Wu, G. H., Chen, J. L., Gao, S. X., Zhan, W. S., Chen, J. H., and Zhang, X. X., 2001, "Intermartensitic Transformation and Magnetic-Field-Induced Strain in $Ni_{52}Mn_{24.5}Ga_{23.5}$ Single Crystals," Appl. Phys. Lett., **79**(8), pp. 1148–1150.
[19] Panovko, Y. G., and Gubanova, I. I., 1965, *Stability and Oscillations of Elastic Systems*, Consultants Bureau, New York, p. 17.
[20] Moon, F. C., and Pao, Y. H., 1968, "Magnetoelastic Buckling of a Thin Plate," ASME J. Appl. Mech., **35**, pp. 53–58.
[21] Moon, F. C., 1970, "The Mechanics of Ferroelastic Plates in a Uniform Magnetic Field," ASME J. Appl. Mech., **37**, pp. 153–158.
[22] Moon, F. C., 1979, "Buckling of a Superconducting Ring in a Toroidal Magnetic Field," ASME J. Appl. Mech., **46**, pp. 151–155.
[23] Moon, F. C., and Swanson, C., 1977, "Experiments on Buckling and Vibration of Superconducting Coils," ASME J. Appl. Mech., **44**, pp. 707–713.
[24] Pao, Y. H., and Yeh, C. S., 1973, "A Linear Theory for Soft Ferromagnetic Elastic Solids," Int. J. Eng. Sci., **11**, pp. 415–436.
[25] Hutter, K., and Pao, Y. H., 1974, "A Dynamic Theory for Magnetizable Elastic Solids With Thermal and Electrical Conduction," J. Elast., **4**(2), pp. 89–114.
[26] Eringen, A. C., 1989, "Theory of Electromagnetic Elastic Plates," Int. J. Eng. Sci., **27**, pp. 363–375.
[27] Miya, K., Takagi, T., and Ando, Y., 1978, "Finite Element Analysis of Magnetoelastic Buckling of Ferromagnetic Beam Plate," ASME J. Appl. Mech.,

**45**, pp. 335–360.
[28] Miya, K., and Uesaka, M., 1982, "An Application of a Finite Element Method to Magneto Mechanics of Superconduction Magnets for Magnetic Reactors," Nucl. Eng. Des., **72**, pp. 275–296.
[29] Van de Ven, A. A. F., 1984, "Magnetoelastic Buckling of a Beam of Elliptic Cross Section," Acta Mech., **51**, pp. 119–183.
[30] Van De Ven, A. A. F., 1978, "Magnetoelastic Buckling of Thin Plates in a Uniform Transverse Magnetic Field," J. Elast., **8**(3), pp. 297–312.
[31] Lieshout, P. H., Rongen, P. M. J., and Van De Ven, A. A. F., 1987, "Variational Principle for Magneto-Elastic Buckling," J. Eng. Math., **21**, pp. 227–252.
[32] Takagi, T., and Tani, J., 1994, "Dynamic Behavior Analysis of a Plate in Magnetic Field by Full Coupling and MMD Methods," IEEE Trans. Magn., **30**(5), pp. 3296–3299.
[33] Xie, H. C., Wang, Zh. Q., and Wang, D. M., 1991, "The Magnetoelastic Buckling of Ferromagnetic Plate With Size Effect," Chinese Journal of Applied Mechanics, **8**(4), pp. 113–117, in Chinese.
[34] Zhou, Y. H., and Zheng, X. J., 1997, "A General Expression of Magnetic Force for Soft Ferromagnetic Plates in Complex Magnetic Fields," Int. J. Eng. Sci., **35**, pp. 1405–1417.
[35] Zhou, Y. H., and Zheng, X. J., 1995, "Development of the Buckling of Soft Ferromagnetic Plate," Adv. Mech., **25**(4), pp. 525–536, in Chinese.
[36] Zheng, X. J., Zhou, Y. H., and Lee, J. S., 1999, "Instability of Superconducting Partial Torus With Two Pin Supports," J. Eng. Mech., **125**, pp. 174–179.
[37] Zheng, X. J., Zhou, Y. H., Wang, X. Z., and Lee, J. S., 1999, "Bending and Buckling of Ferroelastic Plates," J. Eng. Mech., **125**, pp. 180–185.
[38] Zhou, Y. H., and Zheng, X. J., 1997, "Variational Principles of the Magnetoelastic Coupling in Soft Ferromagnetic Plate," Acta Mech. Sin., **18**(2), pp. 95–100, in Chinese.
[39] Zhou, Y. H., and Zheng, X. J., 1996, "A Theoretical Model of Magnetoelastic Buckling for Soft Ferromagnetic Thin Plates," Acta Mech. Sin., **12**(3), pp. 213–224.
[40] Lee, J. S., and Zheng, X. J., 1999, "Bending and Buckling of Superconducting Partial Toroidal Field Coils," Int. J. Solids Struct., **36**, pp. 2127–2141.
[41] Zhou, Y. H., and Miya, K., 1999, "A Theoretical Prediction of Increase of Natural Frequency to Ferromagnetic Plates Under In-Plane Magnetic Fields," J. Sound Vib., **222**(1), pp. 49–64.
[42] Yang, W., Pan, H., Zheng, D., and Cai, Q., 1998, "Buckling of a Ferromagnetic Thin Plate in a Transverse Static Magnetic Field," Chin. Sci. Bull., **43**, pp. 1666–1669.
[43] Yang, W., Pan, H., Zheng, D., and Cai, Q., 1999, "An Energy Method for Analyzing Magnetoelastic Buckling and Bending of Ferromagnetic Plate in Static Magnetic Fields," ASME J. Appl. Mech., **66**, pp. 913–917.
[44] Carman, G. P., and Mitrovic, M., 1996, "Nonlinear Constitutive Relations for Magnetostrictive Materials With Applications to 1-D Problems," J. Intell. Mater. Syst. Struct., **6**, pp. 673–683.
[45] Clark, A. E., Wun-Fogle, M., Restorff, J. B., Lograsso, T. A., Ross, A. R., and Schlagel, D. L., 2000, "Magnetostrictive Galfenol/Alfenol Single Crystal Alloys Under Large Compressive Stresses," *Proceedings of ACTUATOR 2000, Seventh International Conference on New Actuator*, Bremen, Germany, pp. 111–115.
[46] Kvarnsjo, L., and Engdahl, G., 1993, *Differential and Incremental Measurements of Magnetoelastic Parameters of Highly Magnetostrictive Materials: Magnetoelastic Effects and Applications*, L. Lamotte, ed., Elsevier Science, New York, pp. 63–69.
[47] Timme, R. W., 1976, "Magnetomechanical Characteristics of a Terbium-Holmium-Iron Alloy," J. Acoust. Soc. Am., **59**(2), pp. 459–464.
[48] Moffet, M. B., Clark, A. E., Wun-Fogle, M., Linberg, J., Teter, J. P., and McLaughlin, E. A., 1991, "Characterization of Terfenol-D for Magnetostrictive Transducers," J. Acoust. Soc. Am., **89**(3), pp. 1448–1455.
[49] Clatterbuck, D. M., Chan, J. W., and Morris, J. W., Jr., 2000, "The Influence of a Magnetic Field on the Fracture Toughness of Ferromagnetic Steel," Mater. Trans., JIM, **41**(8), pp. 888–892.
[50] Wan, Y., 2002, "Constitutive Relation and Fracture Behavior of Magnetostrictive Materials," Ph.D. thesis, Department of Engineering Mechanics, Tsinghua University, Beijing, in Chinese.
[51] Feng, X., 2002, "Theoretical and Experimental Study of the Constitutive Relation of Soft Ferromagnetic Materials," Ph.D. thesis, Department of Engineering Mechanics, Tsinghua University, Beijing, in Chinese.
[52] Cullity, B. D., 1972, *Introduction to Magnetic Materials*, Addison-Wesley, MA.
[53] Makar, J. M., and Tanner, B. K., 1998, "The Effect of Stress Approaching and Exceeding the Yield Point on the Magnetic Properties of High Strength Pearlitic Steels," NDT & E Int., **31**, pp. 117–127.
[54] Makar, J. M., and Tanner, B. K., 2000, "The Effect of Plastic Deformation and Residual Stress on the Permeability and Magnetostriction of Steels," J. Magn. Magn. Mater., **222**, pp. 291–304.
[55] Stevens, K. J., 2000, "Stress Dependence of Ferromagnetic Hysteresis Loops for Two Grades of Steel," NDT & E Int., **33**, pp. 111–121.
[56] Takahashi, S., Echigoya, J., and Motoki, Z., 2000, "Magnetization Curves of Plastically Deformed Fe Metals and Alloys," J. Appl. Phys., **87**, pp. 805–813.
[57] Devine, M. K., and Jiles, D. C., 1997, "Magnetomechanical Effect in Nickel and Cobalt," J. Appl. Phys., **81**, pp. 5603–5605.
[58] Pearson, J., Squire, P. T., Maylin, M. G., and Gore, J. C., 2000, "Biaxial Stress Effects on the Magnetic Properties of Pure Iron," IEEE Trans. Magn., **36**, pp. 3251–3253.
[59] Clark, A. E., and Belson, H. S., 1972, "Giant Room-Temperature Magnetostrictions in $TbFe_2$ and $DyFe_2$," Phys. Rev. B, **5**, pp. 3642–3644.
[60] Clark, A. E., 1980, *Ferromagnetic Materials*, E. P. Wohlfarth, ed., North-Holland, Amsterdam, p. 531.
[61] Savage, H. T., Clark, A. E., and Powers, J. M., 1975, "Magnetomechanical Coupling and $\Delta E$ Effect in Highly Magnetostrictive Rare Earth-$Fe_2$ Compounds," IEEE Trans. Magn., **11**(5), pp. 1355–1357.
[62] Jiles, D. C., and Thoelke, J. B., 1995, "Magnetization and Magnetostriction in Terbium-Dysprosium-Iron Alloys," Phys. Status Solidi A, **147**, pp. 535–551.
[63] Mei, W., Okane, T., and Umeda, T., 1998, "Magnetostriction of Tb-Dy-Fe Crystals," J. Appl. Phys., **84**, pp. 6208–6216.
[64] Prajapati, K., Greenough, R. D., Wharton, A., Stewart, M., and Gee, M., 1996, "Effect of Cyclic Stress on Terfenol-D," IEEE Trans. Magn., **32**, pp. 4761–4763.
[65] Prajapati, K., Greenough, R. D., and Wharton, A., 1997, "Magnetic and Magnetoelastic Response of Stress Cycled Terfenol-D," J. Appl. Phys., **81**, pp. 5719–5721.
[66] Feng, X., Fang, D.-N., Hwang, K.-C., and Wu, G.-H., 2003, "Ferroelastic Properties of Oriented $Tb_xDy_{1-x}Fe_2$ Polycrystals," Appl. Phys. Lett., **83**(19), pp. 3960–3962.
[67] Dubowik, J., Kudryavtsev, Y. V., and Lee, Y. P., 2004, "Martensitic Transformation in $Ni_2MnGa$ Films: A Ferromagnetic Resonance Study," J. Appl. Phys., **95**(5), pp. 2912–2917.
[68] Dong, J. W., Xie, J. Q., Lu, J., Adelmann, C., Palmstrøm, C. J., Cui, J., Pan, Q., Shield, T. W., James, R. D., and McKernan, S., 2004, "Shape Memory and Ferromagnetic Shape Memory Effects in Single-Crystal $Ni_2MnGa$ Thin Films," J. Appl. Phys., **95**(5), pp. 2593–2600.
[69] Feng, X., Fang, D. N., and Hwang, K. C., 2002, "Mechanical and Magnetostrictive Properties of Fe-Doped Ni52Mn24Ga24 Single Crystals," Chin. Phys. Lett., **19**(10), pp. 1547–1549.
[70] Liang, Y., Kato, H., Taya, M., and Mori, T., 2001, "Straining of NiMnGa by Stress and Magnetic Fields," Scr. Mater., **45**, pp. 569–574.
[71] Jeong, S., Inoue, K., Inoue, S., Koterazawa, K., Taya, M., and Inoue, K., 2003, "Effect of Magnetic Field on Martensite Transformation in a Polycrystalline $Ni_2MnGa$," Mater. Sci. Eng., A, **359**, pp. 253–260.
[72] Yamaguchi, Y., Horiguchi, K., Shindo, Y., Sekiya, D., and Kumagai, S., 2003, "Fracture and Deformation Properties of Ni–Fe Superalloy in Cryogenic High Magnetic Field Environments," Cryogenics, **43**, pp. 469–475.
[73] Wan, Y. P., Fang, D. N., and Soh, A. K., 2003, "Effects of Magnetic Field on Fracture Toughness of Manganese-Zinc Ferrite Ceramics," Mod. Phys. Lett. B, **17**(2), pp. 57–66.
[74] Shindo, Y., Sekiya, D., Narita, F., and Horiguchi, K., 2004, "Tensile Testing and Analysis of Ferromagnetic Elastic Strip With a Central Crack in a Uniform Magnetic Field," Acta Mater., **52**, pp. 4677–4684.
[75] Horiguchi, K., and Shindo, Y., 2004, "A Strain Gage Method for Determination of Magnetic Moment Intensity Factors in Through-Cracked Soft Ferromagnetic Plates," J. Appl. Phys., **96**, pp. 5860–5865.
[76] Shindo, Y., Narita, F., Horiguchi, K., and Komatsu, T., 2006, "Mode I Crack Growth Rate of a Ferromagnetic Elastic Strip in a Uniform Magnetic Field," Acta Mater., **54**, pp. 5115–5122.
[77] Maugin, G. A., and Eringen, A. C., 1972, "Deformable Magnetically Saturated Media, I. Field Equations," J. Math. Phys., **13**(2), pp. 143–155.
[78] Maugin, G. A., and Eringen, A. C., 1972, "Deformable Magnetically Saturated Media, II. Constitutive Theory," J. Math. Phys., **13**(9), pp. 1334–1347.
[79] Jiles, D. C., and Atherton, D. L., 1984, "Microcomputer-Based System for Control of Applied Uni-Axial Stress and Magnetic Field," Rev. Sci. Instrum., **55**(11), pp. 1843–1848.
[80] Jiles, D. C., and Atherton, D. L., 1986, "Theory of Ferromagnetic Hysteresis," J. Magn. Magn. Mater., **61**, pp. 48–60.
[81] Jiles, D. C., 1995, "Theory of the Magnetomechanical Effect," J. Phys. D, **28**, pp. 1537–1547.
[82] Wan, Y. P., Fang, D. N., and Hwang, K.-Ch., 2001, "The Constitutive Relations of the Magnetostrictive Materials," Acta Mech. Sin., **33**(6), pp. 749–757, in Chinese.
[83] Wan, Y. P., Fang, D. N., and Hwang, K.-Ch., 2003, "Nonlinear Constitutive Relations for the Magnetostrictive Materials," Int. J. Non-Linear Mech., **38**, pp. 1053–1065.
[84] Wan, Y. P., Fang, D. N., Soh, A. K., and Hwang, K.-Ch., 2003, "Experimental and Theoretical Study of the Nonlinear Response of a Giant Magnetostrictive Rod," Acta Mech. Sin., **19**(4), pp. 324–329.
[85] Zheng, X. J., and Liu, X. E., 2005, "A Nonlinear Constitutive Model for Terfenol-D Rods," J. Appl. Phys., **97**, p. 053901.
[86] Jia, Z., Liu, W., Zhang, Y., Wang, F., and Guo, D., 2006, "A Nonlinear Magnetomechanical Coupling Model of Giant Magnetostrictive Thin Films at Low Magnetic Fields," Sens. Actuators, A, **128**, pp. 158–164.
[87] Verhoeven, J. D., Ostenson, J. E., and Gibson, E. D., 1989, "The Effect of Composition and Magnetic Beat Treatment on the Magnetostriction of Tb-DyFe Twinned Single Crystals," J. Appl. Phys., **66**(2), pp. 772–779.
[88] Jiles, D. C., and Thoelke, J. B., 1994, "Theoretical Modeling of the Effects of Anisotropy and Stress on the Magnetization and Magnetostriction of TbDyFe," J. Magn. Magn. Mater., **134**, pp. 143–160.
[89] Armstrong, W. D., 1997, "Magnetization and Magnetostriction Processes of $Tb_{0.3}Dy_{0.7}Fe_2$," J. Appl. Phys., **81**, pp. 2321–2326.
[90] Armstrong, W. D., 1997, "Burst Magnetostriction in $Tb_{0.3}Dy_{0.7}Fe_{1.9}$," J. Appl. Phys., **81**(8), pp. 3548–3554.
[91] Maugin, G. A., 1999, *The Thermomechanics of Nonlinear Irreversible Behaviors*, World Scientific, Singapore.
[92] Maugin, G. A., and Sabir, M., 1990, "Mechanical and Magnetic Hardening of

Ferromagnetic Bodies: Influence of Residual Stresses and Application to Nondestructive Testing," Int. J. Plast., **6**, pp. 573–589.
[93] Motogi, S., and Maugin, G. A., 1993, "Elastic Moduli of Demagnetized Polycrystalline Ferromagnets," J. Phys. D, **26**, pp. 1459–1467.
[94] Motogi, S., and Maugin, G. A., 1993, "Nonlinear Stress-Strain Behavior of Multi-Domain Ferromagnets," *Electromagneto-Elastic Materials and Structures*, J. S. Lee, G. A. Maugin, and Y. Shindo, eds., ASME, New York, Vol. AMD-161, pp. 99–114.
[95] Daniel, L., Hubert, O., and Billardon, R., 2004, "Homogenisation of Magnetoelastic Behaviour: From the Grain to the Macro-Scale," Comput. Appl. Math., **23**(2–3), pp. 285–308.
[96] Hirsinger, L., and Lexcellent, C., 2003, "Modelling Detwinning of Martensite Platelets Under Magnetic and (or) Stress Actions on Ni–Mn–Ga Alloys," J. Magn. Magn. Mater., **254–255**, pp. 275–277.
[97] Kiefer, B., and Lagoudas, D. C., 2005, "Magnetic-Field Induced Martensitic Variant Reorientation in Magnetic Shape-Memory Alloys," Philos. Mag., **85**(33–35), pp. 4289–4329.
[98] Bassiouny, E., Ghaleb, A. F., and Maugin, G. A., 1988, "Thermodynamical Formulation for Coupled Electromechanical Hysteresis. I. Basic Equations," Int. J. Eng. Sci., **26**, pp. 1275–1295.
[99] Bassiouny, E., Ghaleb, A. F., and Maugin, G. A., 1988, "Thermodynamical Formulation for Coupled Electromechanical Hysteresis. II. Poling of Ceramics," Int. J. Eng. Sci., **26**, pp. 1297–1306.
[100] Bassiouny, E., and Maugin, G. A., 1989, "Thermodynamical Formulation for Coupled Electromechanical Hysteresis. III. Parameter Identification," Int. J. Eng. Sci., **27**, pp. 975–987.
[101] Bassiouny, E., and Maugin, G. A., 1989, "Thermodynamical Formulation for Coupled Electromechanical Hysteresis. IV. Combined Electromechanical Loading," Int. J. Eng. Sci., **27**, pp. 989–1000.
[102] Kamlah, M., and Tsakmakis, C., 1999, "Phenomenological Modeling of the Nonlinear Electromechanical Coupling in Ferroelectrics," Int. J. Solids Struct., **36**, pp. 669–695.
[103] Kamlah, M., Bohle, U., and Munz, D., 2000, "On a Nonlinear Finite Element Method for Piezoelectric Structures Made of Hysteretic Ferroelectric Ceramics," Comput. Mater. Sci., **19**, pp. 81–86.
[104] Kamlah, M., and Bohle, U., 2001, "Finite Element Analysis of Piezoceramic Components Taking Into Account Ferroelectric Hysteresis Behavior," Int. J. Solids Struct., **38**, pp. 605–633.
[105] Kamlah, M., 2001, "Ferroelectric and Ferroelastic Piezoceramics: Modeling of Electromechanical Hysteresis Phenomena," Continuum Mech. Thermodyn., **13**, pp. 219–268.
[106] Cocks, A. C. F., and McMeeking, R. M., 1999, "A Phenomenological Constitutive Law for the Behavior of Ferroelectric Ceramics," Ferroelectrics, **228**, pp. 219–228.
[107] Feng, X., Fang, D. N., and Hwang, K. C., 2003, "A Phenomenological Constitutive Model for Ferromagnetic Materials Based on Rate-Independent Flow Theory," Key Eng. Mater., **233**, pp. 77–82.
[108] Fang, D. N., Feng, X., and Hwang, K. C., 2002, "A Phenomenological Constitutive Model for Ferromagnetic Materials," *Mechanics of Magnetoelectric Materials and Structures*, J. S. Yang and G. A. Maugin, eds., Shanghai, China.
[109] Fang, D. N., Feng, X., and Hwang, K. C., 2002, "A Phenomenological Model for the Non-Linear Magnetomechanical Coupling in Ferromagnetic Materials," *Proceedings of the Fourth International Conference on Nonlinear Mechanics*, Shanghai, China, pp. 231–234.
[110] Taylor, G. I., 1938, "Plastic Strains in Metals," J. Inst. Met., **62**, pp. 307–324.
[111] Hosford, W. F., 1972, "A Generalized Isotropic Yield Criterion," ASME J. Appl. Mech., **39**, pp. 607–609.
[112] Hill, R., 1990, "Constitutive Modeling of Orthotropic Plasticity in Sheet Metals," J. Mech. Phys. Solids, **38**, pp. 405–417.
[113] Budianski, B., 1984, *Anisotropic Plasticity of Plane-Isotropic Sheets: Mechanics of Materials Behavior*, G. J. Dvorak and R. T. Shield, eds., Elsevier Science, Amsterdam.
[114] Barlat, F., 1987, "Prediction of Tricomponent Plane Stress Yield Surfaces and Associated Flow and Failure Behavior of Strongly Textured FCC Polycrystalline Sheets," Mater. Sci. Eng., **95**, pp. 15–29.
[115] Barlat, F., and Lian, J., 1989, "Plastic Behavior and Stretchability of Sheet Metals. Part I: A Yield Function for Orthotropic Sheets Under Plane Stress Conditions," Int. J. Plast., **5**, pp. 51–66.
[116] Hershey, A. V., 1954, "The Plasticity of an Isotropic Aggregate of Anisotropic Face Centered Cubic Crystals," ASME J. Appl. Mech., **21**, pp. 241–249.
[117] Karafillis, A. P., and Boyce, M. C., 1993, "A General Anisotropic Yield Criterion Using Bounds and a Transformation Weighting Tensor," J. Mech. Phys. Solids, **41**, pp. 1859–1886.
[118] Cherepanov, G. P., 1979, *Brittle Fracture Mechanics*, English ed., translated by K. C. Huang, Science Press, Beijing (1990), in Chinese.
[119] Shindo, Y., 1977, "The Linear Magnetoelastic Problem for a Soft Ferromagnetic Elastic Solid With a Finite Crack," ASME J. Appl. Mech., **44**, pp. 47–50.
[120] Shindo, Y., 1978, "Magnetoelastic Interaction of a Soft Ferromagnetic Elastic Solids With a Penny Shape Crack in a Constant Axial Magnetic Field," ASME J. Appl. Mech., **54**, pp. 291–296.
[121] Shindo, Y., 1980, "Singular Stress in a Soft Ferromagnetic Elastic Solid With Two Coplanar Griffith Cracks," Int. J. Solids Struct., **46**, pp. 537–543.
[122] Shindo, Y., Ohnishi, I., and Tohyama, S., 1997, "Flexural Wave Scattering at a Through Crack in a Conducting Plate Under a Uniform Magnetic Field," ASME J. Appl. Mech., **64**, pp. 828–834.
[123] Shindo, Y., Horiguchi, K., and Shindo, T., 1999, "Magneto-Elastic Analysis of a Soft ferromagnetic Plate With a Through Crack Under Bending," Int. J. Eng. Sci., **37**, pp. 687–702.
[124] Ang, W. T., 1989, "Magnetic Stress in an Anisotropic Soft Ferromagnetic Material With a Crack," Int. J. Eng. Sci., **27**(12), pp. 1519–1526.
[125] Xu, J. X., and Hasebe, N., 1995, "The Stresses in the Neighborhood of a Crack Tip Under Effect of Electromagnetic Forces," Int. J. Fract., **73**, pp. 287–300.
[126] Hang, K. F., and Wang, M. Z., 1995, "Complete Solution of the Linear Magnetoelasticity of the Magnetic Half Space," ASME J. Appl. Mech., **62**, pp. 930–934.
[127] Bagdasarian, G. Y., and Hasanian, D. J., 2000, "Magnetoelastic Interaction Between a Soft Ferromagnetic Elastic Half-Plane With a Crack and a Constant Magnetic Field," Int. J. Solids Struct., **37**, pp. 5371–5383.
[128] Liang, W., Shen, Y., and Fang, D., 2001, "Analysis of the Plane of Soft Ferromagnetic Materials With a Crack," Acta Mech. Sin., **33**, pp. 758–768, in Chinese.
[129] Liang, W., and Shen, Y., 2000, "Magnetoelastic Formulation of Soft Ferromagnetic Elastic Problems With Collinear Cracks: Energy Density Fracture Criterion," Theor. Appl. Fract. Mech., **34**, pp. 49–60.
[130] Liang, W., Shen, Y., and Fang, D. N., 2002, "Magnetoelastic Coupling on Soft Ferromagnetic Solids With an Interface Crack," Acta Mech., **154**(1–4), pp. 1–9.
[131] Sabir, M., and Maugin, G. A., 1996, "On the Fracture of Paramagnets and Soft Ferromagnets," Int. J. Non-Linear Mech., **31**, pp. 425–440.
[132] Fomethe, A., and Maugin, G. A., 1997, "On the Crack Mechanics of Hard Ferromagnets," Int. J. Non-Linear Mech., **33**, pp. 85–95.
[133] Wang, X. M., and Shen, Y. P., 1996, "The Conservation Laws and Path-Independent Integrals With an Application for Linear Electro-Magneto-Elastic Media," Int. J. Solids Struct., **33**(6), pp. 865–878.
[134] Liang, W., Fang, D. N., and Shen, Y., 2002, "Mode I Crack in a Soft Ferromagnetic Material," Fatigue Fract. Eng. Mater. Struct., **25**(5), pp. 519–526.
[135] Liang, W., Fang, D. N., Shen, Y., and Soh, A. K., 2002, "Nonlinear Magnetoelastic Coupling Effects in a Soft Ferromagnetic Material With a Crack," Int. J. Solids Struct., **39**, pp. 3997–4011.
[136] Liang, W., 2002, "Deformation and Fracture of Under Magnetoelastic Coupling," Ph.D. thesis, Department of Engineering Mechanics, Tsinghua University.
[137] Wan, Y. P., Fang, D. N., Soh, A. K., and Hwang, K.-Ch., 2003, "Effects of Magnetostriction on Fracture of a Soft Ferromagnetic Medium With a Crack-Like Flaw," Fatigue Fract. Eng. Mater. Struct., **26**(11), pp. 1091–1102.
[138] Wan, Y. P., Fang, D. N., and Soh, A. K., 2004, "A Small-Scale Magnetic-Yielding Model for an Infinite Magnetostrictive Plane With a Crack-Like Flaw," Int. J. Solids Struct., **41**(22–23), pp. 6129–6146.
[139] Nan, C. W., 1994, "Magnetoelectric Effect in Composites of Piezoelectric and Piezomagnetic Phases," Phys. Rev. B, **50**, pp. 6082–6088.
[140] Huang, J. H., and Kuo, W. S., 1997, "The Analysis of Piezoelectric/Piezomagnetic Composite Materials Containing Ellipsoidal Inclusions," J. Appl. Phys., **81**, pp. 1378–1386.
[141] Huang, J. H., and Chiu, Y. H., 1998, "Magneto-Electro-Elastic Eshelby Tensors for a Piezoelectric-Piezomagnetic Composite Reinforced by Ellipsoidal Inclusions," J. Appl. Phys., **83**, pp. 5364–5370.
[142] Wu, T. L., and Huang, J. H., 2000, "Closed-Form Solutions for the Magnetoelectric Coupling Coefficients in Fibrous Composites With Piezoelectric and Piezomagnetic Phase," Int. J. Solids Struct., **37**, pp. 2981–3009.
[143] Huang, J. H., Nan, C. W., and Li, R. M., 2002, "Micromechanics Approach for Effective Magnetostriction of Composite Materials," J. Appl. Phys., **91**, pp. 9261–9266.
[144] Li, J. Y., and Dunn, M. L., 1998, "Anisotropic Coupled-Field Inclusion and Inhomogeneity Problems," Philos. Mag. A, **77**, pp. 1341–1350.
[145] Li, J. Y., 2000, "Magnetoelectroelastic Multi-Inclusion and Inhomogeneity Problems and Their Applications in Composite Materials," Int. J. Eng. Sci., **38**, pp. 1993–2011.
[146] Feng, X., Fang, D. N., and Hwang, K. C., 2002, "An Analytical Model for Predicting Effective Magnetostriction of Magnetostrictive Composites," Mod. Phys. Lett. B, **16**(28–29), pp. 1107–1114.
[147] Feng, X., Fang, D. N., Soh, A. K., and Hwang, K. C., 2003, "Predicting Effective Magnetostriction and Moduli of Magnetostrictive Composites by Using the Double-Inclusion Method," Mech. Mater., **35**, pp. 623–631.
[148] Feng, X., Fang, D. N., and Hwang, K. C., 2002, "An Extended Double-Inclusion Model for Predicting Overall Elastic Properties and Magnetostriction of Magnetostrictive Composites," *Proceedings of Mesomechanics*, Denmark.
[149] Pinkerton, E. E., Capehart, T. W., Herbst, J. F., Brewer, E. G., and Murphy, C. B., 1997, "Magnetostrictive SmFe2/Metal Composites," Appl. Phys. Lett., **70**, pp. 2601–2603.
[150] Chen, Y., Snyder, J. E., Schwichtenberg, C. R., Dennis, K. W., Falzgraf, D. K., McCallum, R. W., and Jiles, D. C., 1999, "Effect of the Elastic Modulus of the Matrix on Magnetostrictive Strain in Composites," Appl. Phys. Lett., **74**, pp. 1159–1161.
[151] Duenas, T. A., and Carman, G. P., 2000, "Large Magnetostrictive Response of Terfenol-D Resin Composites," J. Appl. Phys., **87**, pp. 4696–4701.
[152] Guo, Z. J., Busbridge, S. C., Piercy, A. R., Zhang, Z. D., Zhao, X. G., and Wang, B. W., 2001, "Effective Magnetostriction and Magnetomechanical Coupling of Terfenol-D Composites," Appl. Phys. Lett., **78**, pp. 3490–3492.

[153] Ryu, J., Priya, S., Carazo, A. V., and Uchino, K., 2001, "Effect of the Magnetostrictive Layer on Magnetoelectric Properties in Lead Zirconate Titanate/Terfenol-D Laminate Composites," J. Am. Ceram. Soc., **84**, pp. 2905–2908.
[154] Nan, C. W., 1998, "Effective Magnetostriction of Magnetostrictive Composites," Appl. Phys. Lett., **72**, pp. 2897–2899.
[155] Nan, C. W., and Weng, G. J., 1990, "Influence of Microstructural Features on the Effective Magnetostriction of Composite Materials," Phys. Rev. B, **60**, pp. 6723–6730.
[156] Nan, C. W., Huang, Y., and Weng, G. J., 2000, "Effect of Porosity on the Effective Magnetostriction of Polycrystals," J. Appl. Phys., **88**, pp. 339–343.
[157] Armstrong, W. D., 2000, "Nonlinear Behavior of Magnetostrictive Particle Actuated Composite Materials," J. Appl. Phys., **87**(6), pp. 3027–3031.
[158] Armstrong, W. D., 2000, "The Non-Linear Deformation of Magnetically Dilute Magnetostrictive Particulate Composites," Mater. Sci. Eng., A, **285**, pp. 13–17.
[159] Herbst, J. W., Capehart, T. W., and Pinkerton, F. E., 1997, "Estimating the Effective Magnetostriction of a Composite: A Simple Model," Appl. Phys. Lett., **70**, pp. 3041–3043.
[160] Hori, M., and Nemat-Nasser, S., 1993, "Double-Inclusion Model and Overall Moduli of Multi-Phase Composites," Mech. Mater., **14**, pp. 189–206.
[161] Hori, M., and Nemat-Nasser, S., 1994, "Double-Inclusion Model and Overall Moduli of Multi-Phase Composites," ASME J. Eng. Mater. Technol., **116**, pp. 305–309.
[162] Wan, Y. P., Zhong, Z., and Fang, D. N., 2004, "Permeability Dependence of the Effective Magnetostriction of Magnetostrictive Composites," J. Appl. Phys., **95**(6), pp. 3099–3110.

***Daining Fang*** *is a "Yangtze River" Chair Professor, Head of Institute of Solid Mechanics, Tsinghua University, Head of "Failure Mechanics," Key Laboratory of Ministry of Education of China, and Vice Chairman of the Chinese Society of Theoretical and Applied Mechanics. His research fields are (1) electromagnetic solid mechanics and mechanics for microelectronics devices, (2) micromechanics and physically based continuum models with length scales, and (3) strengthening and toughening of advanced materials. He has published more than 100 internationally refereed journal papers. He is in charge of several national research projects funded by the National Natural Science Foundation of China (NSFC), by the Ministry of Science and Technology of China, and by the Ministry of Education of China. He received an award as a National Outstanding Youth Scientist by NSFC, an award of Trans-century Youth Talent by the Ministry of Education of China, and a National Natural Science Prize.*

***Yongping Wan*** *is currently an associate professor of solid mechanics in School of Aerospace Engineering and Applied Mechanics at Tongji University, Shanghai, China. He received his Ph.D. from the Department of Engineering Mechanics at Tsinghua University, Beijing, China in January 2003. He went to the Tohoku University, Japan as a visiting scholar from June 2005 to March 2006. His major interests include the mechanics of electromagnetic solids, smart materials, and structures. He has authored 20 refereed journal and conference scientific papers.*

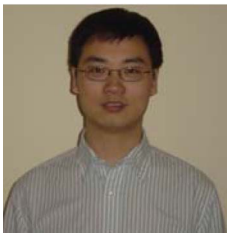

***Xue Feng*** *received a BS degree from Chongqing University in July 1998 and a Ph.D. degree from Tsinghua University in January 2003. He did research in the University of Illinois at Urbana-Champaign as a postdoctoral associate from September 2004 to July 2007, and in California Institute of Technology as a visiting postdoctoral scholar from July 2005 to January 2007. He currently works in the Department of Engineering Mechanics, Tsinghua University as an associate professor. His research focuses on thin film, fracture mechanics, experimental mechanics, and electromagnetomechanics of solids.*

***Ai Kah Soh*** *obtained his Ph.D. from the University of Surrey (UK) in 1980. He is currently a professor in the Department of Mechanical Engineering, The University of Hong Kong. His research interest includes constitutive theory and toughening mechanisms of advanced materials, micro/nano mechanics of deformation and fracture, electromagnetic solid mechanics, and multiscale modeling.*